

Electroweak Phase Transition in the Z_3 -invariant NMSSM

Implications of LHC and Dark matter Searches and Prospects of Detecting the Gravitational Waves

Arindam Chatterjee,^a Asesh Krishna Datta^b and Subhojit Roy^{b,c}

^a*Department of Physics, School of Natural Sciences, Shiv Nadar University, Gautam Buddha Nagar, Uttar Pradesh 201314, India*

^b*Harish-Chandra Research Institute, A CI of Homi Bhabha National Institute, Chhatnag Road, Jhansi, Prayagraj (Allahabad) 211019, India*

^c*Regional Centre for Accelerator-based Particle Physics, Harish-Chandra Research Institute, Prayagraj (Allahabad) 211019, India*

E-mail: arindam.chatterjee@snu.edu.in, asesh@hri.res.in,
subhojitroy@hri.res.in

ABSTRACT: We study in detail the viability and the patterns of a strong first-order electroweak phase transition as a prerequisite to electroweak baryogenesis in the framework of Z_3 -invariant Next-to-Minimal Supersymmetric Standard Model (NMSSM), in the light of recent experimental results from the Higgs sector, dark matter (DM) searches and those from the searches of the lighter chargino and neutralinos at the Large Hadron Collider (LHC). For the latter, we undertake thorough recasts of the relevant, recent LHC analyses. With the help of a few benchmark scenarios, we demonstrate that while the LHC has started to eliminate regions of the parameter space with relatively small μ_{eff} , that favors the coveted strong first-order phase transition, rather steadily, there remains phenomenologically much involved and compatible regions of the same which are yet not sensitive to the current LHC analyses. It is further noted that such a region could also be compatible with all pertinent theoretical and experimental constraints. We then proceed to analyze the prospects of detecting the stochastic gravitational waves, which are expected to arise from such a phase transition, at various future/proposed experiments, within the mentioned theoretical framework and find them to be somewhat ambitious under the currently projected sensitivities of those experiments.

KEYWORDS: Beyond Standard Model, Supersymmetry Phenomenology, Cosmology of Theories beyond the Standard Model, Electroweak Phase transition, Gravitational wave

Contents

1	Introduction	1
2	The theoretical framework: the Z_3-NMSSM	4
2.1	The Higgs sector	5
2.2	The electroweakino sector	6
3	EWPT in the NMSSM: a prerequisite to EWBG and its implications	7
3.1	Generalities of EWBG	7
3.2	Study of EWPT in the Z_3 -NMSSM	9
3.2.1	Effective Higgs potential at finite-temperature	9
3.2.2	Target region of the NMSSM parameter space	12
3.3	Production of GW from first-order phase transition	14
4	Results	17
4.1	Constraints from various sectors	17
4.2	Choice and study of benchmark scenarios	20
4.3	Studying the benchmark scenarios	21
4.3.1	Disallowed scenarios with low μ_{eff}	22
4.3.2	Allowed benchmark scenarios with successful nucleation	26
4.3.3	Prospects of GW detection	32
5	Summary and outlook	34
6	Acknowledgments	36
	Appendices	37
A	Matching the NMSSM parameters to those in the THDMS potential	37
B	RGEs in the THDMS	38
C	Field-dependent masses and the daisy corrections	39

1 Introduction

Electroweak phase transition (EWPT), leading to electroweak symmetry breaking (EWSB), is central to the process of baryogenesis at the electroweak scale or Electroweak Baryogenesis (EWBG) [1–3] which can explain the observed preponderance of (primordial) baryons over antibaryons, the so-called Baryon Asymmetry in the (present-day) Universe (BAU).

The customary measure of BAU, Y_B , is the ratio of the difference between baryon and antibaryon densities (n_B and $n_{\bar{B}}$, respectively) and the entropy density (s), i.e., $Y_B = (n_B - n_{\bar{B}})/s$. Its most precise value to date ($Y_B = 8.65 \pm 0.09 \times 10^{-11}$) comes from the measurement at the Planck experiment [4] of the baryon acoustic oscillations that it gives rise to in the power spectrum of the cosmic microwave background (CMB).

For baryogenesis to take place, the much celebrated set of following three Sakharov criteria [5] are to be necessarily met: (i) baryon number non-conservation (\mathcal{B}), (ii) C and CP violations (\mathcal{C} , \mathcal{CP}) and (iii) departure from thermal equilibrium. EWBG is no exception. However, reference [5] was found to be rather prescient about scenarios based on Grand Unified Theories (GUTs) [6–8].

BAU can also be realized in some other motivated extensions of the Standard Model (SM) of particle physics where the same arises from a (s)lepton asymmetry (i.e., via leptogenesis) [9–11] in a supersymmetric (SUSY) framework or via the Affleck-Dine mechanism [12, 13] or even with the help of gravitational effects [14]. Among all these, EWBG has attracted special attention as it necessarily invokes physics beyond the Standard Model (BSM) down at around the electroweak (EW) scale which is being (and will be) intensely probed at various experiments including at the colliders. Naturally, EWPT, as an essential trigger for EWBG, has continued to be an area of active research [8, 15–20].

However, at temperatures as low as around the weak scale, while \mathcal{B} (as anomaly effects [21], via finite-temperature ‘sphaleron’ transitions) and \mathcal{C} and \mathcal{CP} (induced by the CKM phase) could be present in a scenario with electroweak interactions like the SM, it is difficult to find a departure from thermal equilibrium [18]. EWPT can salvage the situation if it is a first-order phase transition (FOPT) and that also of a ‘strong’ nature. Such a transition proceeds in steps starting with the nucleation of bubbles of the broken phase in the cosmological plasma of the symmetric phase, followed by their expansions and eventual collisions and mergers until the whole space is engulfed by the broken phase. The process is violent enough to trigger local departures from thermal equilibrium in the vicinity of the walls of the rapidly expanding bubbles in the plasma.

Unfortunately, however, an FOPT (and hence EWBG) cannot be realized in the SM given that the observed SM-like Higgs boson is too heavy ($m_{h_{\text{SM}}} \approx 125$ GeV [22, 23]) for the purpose [24, 25]. This is since such a value of $m_{h_{\text{SM}}}$ signifies a large enough Higgs quartic coupling (λ_H) which virtually suppresses the term cubic in the Higgs fields in the ‘effective’ (higher-order) Higgs (scalar) potential. This deprives the potential of a crucial bump (as it varies with the field(s)) which is essential for an FOPT. Also, \mathcal{CP} from the CKM phase in the SM is proven inadequate for generating enough chiral asymmetries [26–29] for \mathcal{B} to occur. Hence SM, as such, cannot lead to EWBG.

It is well known that popular SUSY extensions of the SM, viz., the Minimal SUSY SM (MSSM) and its next-to-minimal incarnation (NMSSM), a priori, provide the right setup [30, 31] for EWBG. In the presence of an extended Higgs sector in these scenarios and other scalar degrees of freedom (in particular, the top squarks) in their spectra, an effective Higgs potential of the right kind for an FOPT to occur can be found. Furthermore, some new Lagrangian parameters could now be the sources of additional \mathcal{CP} that triggers \mathcal{B} thus

facilitating the generation of BAU. However, since the MSSM parameter space favoring a strong first-order electroweak phase transition (SFOEWPT) has now got highly disfavored (as it requires rather light top squarks [32] which are constrained by the LHC searches), the NMSSM (and its variants) has stolen the limelight.

EWPT in the NMSSM is rather appealing because of the presence of a gauge singlet scalar field which helps generate a barrier between the symmetric and the broken electroweak phases of the Higgs potential that is required for an FOPT. Unlike in the MSSM, such a barrier may now arise even at the tree level and at zero-temperature thanks to the presence of cubic terms in the Higgs potential. Thus, the dimensionful couplings in these cubic terms in the soft Lagrangian involving the singlet scalar field and the doublet Higgs fields could play important roles in altering the barrier in favor of an SFOEWPT [31].

Naturally, there has been a continued activity over the past decades exploring myriad aspects and possibilities of EWPT in the NMSSM. In particular, some of these shed light on how SFOEWPT, the experimental constraints on the dark matter (DM) observables and the spectrum of the singlet- and/or doublet-like scalars are connected across the NMSSM parameter space [33–35], its region over which simultaneous compatibility of SFOEWPT and the Galactic Centre Excess (GCE) can be found [36] while some others present analyses of EWBG in the presence of SFOEWPT [35, 37–41].

Further, a recent study [52] has undertaken a detailed probe into the patterns of phase transitions, based on calculations of critical temperature, that are possible over an extended region of the Z_3 -NMSSM parameter space using the package `PhaseTracer` [53] which is designed specifically for the purpose. Subsequently, in the context of such a scenario (in the so-called ‘alignment without decoupling limit’ in the Higgs sector), it has been demonstrated [54] with the help of the package `CosmoTransitions` [55] that ensuring a successful nucleation of a bubble of the broken electroweak phase is more crucial than just confirming the presence of a critical temperature for an FOPT.

In both the studies mentioned above [52, 54], only the Higgs-related constraints from the LHC and the bounds on the chargino-neutralino (electroweakinos) sectors from the LEP experiments are considered. Stringent bounds on the latter sector from the recent LHC studies and those on the DM observables, viz., the DM relic abundance and the DM direct detection (DMDD) rates for both the spin-independent (SI) and the spin-dependent (SD) cases, are, however, not imposed in either of these works. As mentioned there, such considerations are perfectly justified in dedicated studies of EWPT in which neither the properties of these electroweakinos in general, nor those of the DM are of much practical concern.

Going beyond, our goal in this work is to examine the prospects of SFOEWPT in the Z_3 -NMSSM once the latest constraints from the LHC and the DM sector are included in the analysis and their implications thereof. Given that these constraints are already known to be intricately connected over the Z_3 -NMSSM parameter space, such an exercise takes off by throwing the physics of EWPT into the mix. Together, these are likely to shed more light on the viability of EWBG in such a framework. We would, however (as is customary in such studies), remain agnostic about the extra sources of \mathcal{C} , \mathcal{CP} or how \mathcal{B} is achieved with the understanding that those could always be arranged optimally.

It is perhaps straightforward to imagine [37] that the issues in the DM, the LHC and the EWPT sectors are all connected via the higgsino ‘portal’. For, the effective higgsino mass parameter (μ_{eff}) of the scenario could affect all those sectors significantly, especially, intricately as there are a few other model parameters that appear both in the electroweakino and the Higgs sectors. As we will see, such a connection gives rise to a tantalizing possibility that relatively light higgsinos with masses under a few hundred GeV, in the presence of an even lighter singlino and/or a bino, with or without accompanying singlet-like scalar(s), might have been, somewhat comfortably, escaping their searches at the LHC even at this matured stage of the experiment. In particular, we seek to explore how small a μ_{eff} could still be viable in view of the current experimental constraints given that it is somewhat motivated by ‘naturalness’ and, at the same time, is preferred by SFOEWPT and hence by EWBG.

On the other side of the proceedings, the dynamics of the nucleated bubbles could generate gravitational waves (GW) [56–63]. These would be stochastic in nature and could be detected by dedicated ground-based and space-borne experiments. Note that in the SM, EWPT is of a cross-over type. Hence it does not produce any GW in the early Universe. That is why the detection of such a stochastic background would likely to hint physics beyond the SM (BSM). In the context of the NMSSM, the production of such GW has recently been studied [37, 38, 45, 47]. In this work, we also present, for a chosen set of scenarios, the prospects of detection of such a GW background in future experiments.

The present work is organized as follows. In section 2 we briefly discuss the Z_3 -NMSSM scenario with a focus on its scalar and electroweakino sectors which the present study is particularly sensitive to. Section 3 summarizes the generalities of EWBG by stressing SFOEWPT as its prerequisite. A schematic details of EWPT is then presented in the Z_3 -NMSSM scenario, matched to the THDSM, in terms of the finite-temperature effective (scalar) potential and the target region of the parameter space for our present study is outlined. A brief discussion on the mechanism of GW production in FOPT follows where we collect its basic theoretical ingredients. In section 4 we present our results where we delineate the relevant region of the parameter space, choose a few benchmark scenarios for our purpose that meet all primary constraints, show that some of these do survive explicit recasts of some recent, relevant LHC analyses (first of its kind, in the current context) and demonstrate in some detail how SFOEWPT is realized in each such case which together underscores an overall preference for a relatively small μ_{eff} . Prospects of detecting the GWs at future experiments in these viable scenarios are then presented. In section 5 we conclude with an outlook for the future. A three-part appendix outlines the key details of the implementation of our scenario in `CosmoTransitions`.

2 The theoretical framework: the Z_3 -NMSSM

In this section we discuss the theoretical framework, i.e., the Z_3 -NMSSM with conserved R -parity, by outlining the superpotential, the soft SUSY breaking Lagrangian of the scenario followed by a brief description of its Higgs (scalar) and electroweakino sectors, that are relevant for the present work, at the tree-level.

The superpotential is given by [48]

$$\mathcal{W} = \mathcal{W}_{\text{MSSM}}|_{\mu=0} + \lambda \widehat{S} \widehat{H}_u \cdot \widehat{H}_d + \frac{\kappa}{3} \widehat{S}^3, \quad (2.1)$$

where $\mathcal{W}_{\text{MSSM}}|_{\mu=0}$ is the MSSM superpotential with its higgsino mass term (the μ -term) dropped, \widehat{H}_u , \widehat{H}_d and \widehat{S} are the $SU(2)$ Higgs doublet superfields and the gauge singlet superfield, respectively, and ‘ λ ’ and ‘ κ ’ are dimensionless parameters. The (real) scalar component of the singlet superfield \widehat{S} assumes a non-zero vacuum expectation value (vev) v_s during EWPT thus generating an effective μ -term as $\mu_{\text{eff}} = \lambda v_s / \sqrt{2}$. Correspondingly, the soft SUSY-breaking Lagrangian is given by

$$-\mathcal{L}^{\text{soft}} = -\mathcal{L}_{\text{MSSM}}^{\text{soft}}|_{B\mu=0} + m_S^2 |S|^2 + (\lambda A_\lambda S H_u \cdot H_d + \frac{\kappa}{3} A_\kappa S^3 + \text{h.c.}), \quad (2.2)$$

where m_S is the soft SUSY-breaking mass of the singlet scalar field, ‘ S ’, H_u and H_d are the doublet Higgs fields and A_λ and A_κ are the NMSSM-specific trilinear soft couplings with mass dimension one.

2.1 The Higgs sector

The tree-level Higgs (scalar) potential of the Z_3 -NMSSM takes the following form:

$$V_{\text{tree}}^{\text{NMSSM}} = V_F + V_D + V_{\text{soft}}, \quad (2.3)$$

where V_F , V_D and V_{soft} represent contributions from the F - and the D -terms and the soft SUSY-breaking terms, respectively and are given by

$$V_F = |\lambda S|^2 (|H_u|^2 + |H_d|^2) + |\lambda H_u \cdot H_d + \kappa S^2|^2, \quad (2.4)$$

$$V_D = \frac{1}{8} g^2 (|H_u|^2 - |H_d|^2)^2 + \frac{1}{2} g_2^2 |H_u^\dagger H_d|^2, \quad (2.5)$$

$$V_{\text{soft}} = m_{H_u}^2 |H_u|^2 + m_{H_d}^2 |H_d|^2 + m_S^2 |S|^2 + (\lambda A_\lambda S H_u \cdot H_d + \frac{1}{3} \kappa A_\kappa S^3 + \text{h.c.}), \quad (2.6)$$

where $g^2 = (g_1^2 + g_2^2)/2$ and g_1 and g_2 are, respectively, the $U(1)$ and the $SU(2)$ gauge couplings. In our present study, we consider the Lagrangian parameters $\lambda, \kappa, A_\lambda$ and A_κ to be real. The complex scalar fields can be expressed as

$$H_u = \begin{pmatrix} H_u^+ \\ \frac{1}{\sqrt{2}} (h_u + i a_u) \end{pmatrix}, \quad H_d = \begin{pmatrix} \frac{1}{\sqrt{2}} (h_d + i a_d) \\ H_d^- \end{pmatrix}, \quad S = \frac{1}{\sqrt{2}} (s + i \sigma), \quad (2.7)$$

where $\langle h_u \rangle = v_u$, $\langle h_d \rangle = v_d$ and $\langle s \rangle = v_s$ are the $vevs$ of the real components (CP -even) of the neutral scalar fields that refer to the tree-level scalar potential at zero temperature. Note that $\sqrt{v_u^2 + v_d^2} = v \simeq 246$ GeV with $\tan \beta = v_u / v_d$ and $\mu_{\text{eff}} = \lambda v_s / \sqrt{2}$.

On electroweak symmetry breaking (EWSB), the doublet and the singlet scalars could mix and the physical Higgs states arise. The tree-level mass-squared matrices for the CP -even, the CP -odd and the charged scalars in the bases $\{h_d, h_u, s\}$, $\{a_d, a_u, \sigma\}$ and $\{H_u^+, H_d^{-*}\}$, respectively, are obtained by expanding the scalar potential of equation 2.3 around v_d, v_u

and v_s (see equation A.1) and taking its double derivatives with respect to the scalar fields of the involved types. Diagonalizations of these mass-squared matrices lead to three CP -even, two CP -odd and two charged physical Higgs states. One of the lighter CP -even states has to be the observed SM-like Higgs boson, h_{SM} . Thus, there is the interesting phenomenological possibility that one scalar state from each of the CP -even and the CP -odd sectors is light and is singlet-like (h_s and a_s) and hence might have managed to escape detection at various collider experiments. Their heavier counterparts (H and A) would then be similar to those found in the MSSM. Note that these Higgs masses depend on the cubic couplings in which the parameters A_λ and A_κ appear and these are found to play important roles in achieving FOEWPT. Also, for an FOEWPT (and hence for an EWBG), of particular interest is the effective scalar potential at finite-temperature. We discuss its salient aspects in section 3.

2.2 The electroweakino sector

The neutralino sector of the Z_3 -NMSSM consists of five neutralinos which are mixtures of bino (\tilde{B}), wino (\tilde{W}_3^0), two higgsinos ($\tilde{H}_d^0, \tilde{H}_u^0$) and a singlino (\tilde{S}) which is the fermionic component of the singlet superfield \hat{S} appearing in the superpotential of equation 2.1. The symmetric, real 5×5 neutralino mass-matrix, \mathcal{M}_0 , in the gauge (weak) basis $\psi_0 \equiv \{\tilde{B}, \tilde{W}_3^0, \tilde{H}_d^0, \tilde{H}_u^0, \tilde{S}\}$, is given by [48]

$$\mathcal{M}_0 = \begin{pmatrix} M_1 & 0 & -\frac{g_1 v_d}{2} & \frac{g_1 v_u}{2} & 0 \\ \dots & M_2 & \frac{g_2 v_d}{2} & -\frac{g_2 v_u}{2} & 0 \\ \dots & \dots & 0 & -\mu_{\text{eff}} & -\frac{\lambda v_u}{\sqrt{2}} \\ \dots & \dots & \dots & 0 & -\frac{\lambda v_d}{\sqrt{2}} \\ \dots & \dots & \dots & \dots & \sqrt{2\kappa v_s} \end{pmatrix}, \quad (2.8)$$

where M_1 (M_2) is the soft SUSY-breaking mass for the bino (wino). The [5,5] element of \mathcal{M}_0 is the singlino mass term, $m_{\tilde{S}} = \sqrt{2\kappa v_s}$. \mathcal{M}_0 can be diagonalized by an orthogonal 5×5 matrix ‘ N ’, i.e.,

$$N\mathcal{M}_0N^T = \mathcal{M}_D = \text{diag}(m_{\chi_1^0}, m_{\chi_2^0}, m_{\chi_3^0}, m_{\chi_4^0}, m_{\chi_5^0}), \quad (2.9)$$

when the neutralino mass eigenstates, χ_i^0 , are given in terms of the weak eigenstates, ψ_j^0 , by

$$\chi_i^0 = N_{ij}\psi_j^0, \quad \text{with } i, j = 1, 2, 3, 4, 5, \quad (2.10)$$

and χ_i^0 's are ordered in increasing mass as ‘ i ’ increases. In this study, we set M_2 large. Thus, the heaviest neutralino (χ_5^0) is almost a pure wino and is indeed heavy with a mass $m_{\chi_5^0} \approx M_2$. Hence the wino practically decoupled when \mathcal{M}_0 effectively reduces to a (4×4) matrix. The scenario conserves R -parity which is odd for the SUSY excitations. Thus, the lightest SUSY particle (LSP) which is taken to be the lightest neutralino (χ_1^0) in this work turns stable and can be a good DM candidate.

The chargino sector of the Z_3 -NMSSM is exactly the same as in the MSSM but for $\mu \rightarrow \mu_{\text{eff}}$. The 2×2 chargino mass-matrix, \mathcal{M}_C , in the gauge bases $\psi^+ = \{-i\widetilde{W}^+, \widetilde{H}_u^+\}$ and $\psi^- = \{-i\widetilde{W}^-, \widetilde{H}_d^-\}$, is given by [48]

$$\mathcal{M}_C = \begin{pmatrix} M_2 & \frac{g_2 v_u}{\sqrt{2}} \\ \frac{g_2 v_d}{\sqrt{2}} & \mu_{\text{eff}} \end{pmatrix}. \quad (2.11)$$

As in the MSSM, \mathcal{M}_C can be diagonalized by two 2×2 unitary matrices ‘ U ’ and ‘ V ’, i.e.,

$$U^* \mathcal{M}_C V^\dagger = \text{diag}(m_{\chi_1^\pm}, m_{\chi_2^\pm}), \quad \text{with } m_{\chi_1^\pm} < m_{\chi_2^\pm}, \quad (2.12)$$

where, in the present work, χ_1^\pm (χ_2^\pm) is higgsino-like (wino-like) given that we set M_2 large.

As we will find, a relatively light singlino-dominated neutralino, which, at times, can be the LSP, has a special context in this work. The latter requires $|\sqrt{2}\kappa v_s| < |\mu_{\text{eff}}|, |M_1|$. Given $v_s = \sqrt{2}\mu_{\text{eff}}/\lambda$, this then requires ‘ κ ’ to be on the smaller side (with $|\kappa| < 2\lambda$) which is just what an SFOEWPT prefers. Furthermore, the mutual hierarchy among these electroweakinos would have important implications for their phenomenologies at the LHC.

3 EWPT in the NMSSM: a prerequisite to EWBG and its implications

In this section we take a quick tour into the generalities of EWBG and its association with (FO)EWPT followed by a brief discussion of the latter in the Z_3 -NMSSM. Some relevant analytical details which have gone into our implementations of the scenario in `CosmoTransitions` are deferred to the appendices.

3.1 Generalities of EWBG

Like any successful model of baryogenesis, EWBG also requires the three Sakharov criteria, as mentioned in the Introduction, are to be fulfilled. As noted there, EWBG exploits FOEWPT which triggers electroweak symmetry breaking (EWSB) at the characteristic energy-scale (~ 100 GeV). In the process, important roles are played by the radiative [64] and finite-temperature [29] corrections to the Higgs potential. For the FOEWPT, the latter ensures an optimal evolution of the potential as the Universe expands and cools down from an early, hot (radiation-dominated) epoch where the electroweak symmetry was still intact [65, 66].

A possible FOEWPT is envisaged when there appear (at least) two distinct local minima of the finite-temperature effective Higgs potential, separated already by a barrier when the temperature (T) of the Universe is such that $T > T_c$, where T_c is the so-called ‘critical temperature’, i.e., the temperature at which the two minima become degenerate, still separated by a barrier. One such minimum is a trivial one with a vanishing potential for null values of the participating scalar fields where the electroweak symmetry is (trivially) preserved. For $T < T_c$, the true (global) minimum emerges with a smaller value of the potential for finite field-values in the broken phase and the field(s) at the trivial (local) minimum (the false vacuum) naturally tries to tunnel to the true one [67–69].

The tunneling process is efficiently modeled in terms of a bubble of the broken electroweak phase nucleated locally in the cosmological plasma (in which the electroweak symmetry is intact) that starts growing as the rate of nucleation (Γ_B , per unit volume) exceeds the same for the Hubble expansion. A bubble, once formed, continues to expand, collide and coalesce with other bubbles growing in the plasma until a giant one, formed this way, engulfs the whole space thus making EWSB permeate all over. At finite-temperatures (T), in the semi-classical approximation, $\Gamma_B \propto T^4 \exp(-S_3(T)/T)$ [70–72], where $S_3(T)$ is the effective three-dimensional Euclidean action evaluated at the (“bounce”) solution of the classical field equation. The minimal requirement for a successful completion of an EWPT requires the bubble nucleation rate to be one per Hubble volume per Hubble time. This is met when $\frac{S_3(T)}{T} \simeq 140$ [69, 73, 74]. The corresponding nucleation temperature T_n ($\lesssim T_c$) is the highest temperature for which $\frac{S_3(T)}{T} \lesssim 140$ is satisfied, as the Universe cools down. We use `CosmoTransitions` [55] to calculate this bounce solution by employing path deformation method.

Along the way, for EWBG to take place, the three Sakharov conditions are met and play their roles [1, 8] in the following manner.

- The SM can give rise to \mathcal{B} [21] thanks to the triangle anomaly [75, 76]. This is described in terms of the vacuum configurations of the static gauge field of the unbroken $SU(2)_L$ gauge theory in which alternating degenerate vacua with integer-value Chern-Simons numbers carry different baryon numbers and are separated by potential barriers whose constant height (E_{sph}) is given by static solutions that are known as “sphalerons” [77–79]. At finite-temperatures \mathcal{B} occurs via sphaleron transitions (hopping of the barriers) [1] from one vacuum to another. The transition rate (per unit volume per unit time) in the symmetric phase scales as T^4 , while in the broken phase, the same is suppressed exponentially as $\exp(-\frac{E_{\text{sph}}(T)}{T})$ [80–82]. The same mechanism works in the SUSY extensions of the SM, including the NMSSM [83, 84].
- Complementary sphaleron-induced processes would generate similar excesses in baryons and antibaryons thus leading to a null baryon asymmetry. When the underlying theory possesses \mathcal{CP} , preferential scattering of fermions with a specific chirality in the symmetric phase with the expanding bubble wall could generate both CP and C asymmetries in the particle number densities in that phase thus biasing the sphalerons there to generate more baryons than antibaryons [85, 86]. As noted in the Introduction, while SM does not have a strong enough source of \mathcal{CP} , SUSY extensions like the NMSSM have new sources of \mathcal{CP} in the form of phases in the extended Higgs sector and/or in the gaugino masses etc., which make up for the deficit.
- Even in the presence of \mathcal{B} , \mathcal{C} and \mathcal{CP} , the equilibrium average of net baryon number vanishes as a consequence of CPT -invariance [16, 17]. Thus, to create a maintainable baryon asymmetry in the front of the bubble wall, the cosmological plasma in its vicinity should depart from thermal equilibrium. Such a departure is generically realized under FOEWPT when the nucleated bubble rapidly expands through the plasma.

- Some fraction of this baryon asymmetry thus generated in the symmetric phase subsequently diffuses into the broken phase [8, 19, 87] thanks to the motion of the bubble wall. For $T < T_c$ (more precisely, for $T < T_n$), $\frac{E_{\text{sph}}(T)}{T}$ is large in the broken phase and the exponential suppression in the rate of sphaleron transitions, as mentioned under the first item above, kicks in. Quantitatively, for $\frac{\phi_n}{T_n} \equiv \gamma_{\text{EW}} \gtrsim 1$,¹ i.e., for a “strong” FOEWPT, where $\phi_n = \langle \phi \rangle_{T_n}$ in the broken phase [73, 88, 89], this rate per unit volume falls out of equilibrium thus rendering the rate of \mathcal{B} too slow to wash out the baryon-asymmetry that has sneaked into the broken phase. This completes the process of successful baryogenesis.

Given that a FOEWPT is central to the process of EWBG, we briefly review the same in the next subsection in the context of Z_3 -NMSSM.

3.2 Study of EWPT in the Z_3 -NMSSM

In this section we outline the formulation of EWPT in the Z_3 -NMSSM and discuss the viability of SFOEWPT that facilitates EWBG over the model parameter space. We assume that there is no spontaneous or explicit \mathcal{CP} in the Higgs sector.

3.2.1 Effective Higgs potential at finite-temperature

To study the viability of SFOEWPT in the Z_3 -NMSSM, we start with the description of the effective potential for the Higgs sector. The zero-temperature radiatively corrected (at one-loop) effective potential for the (CP -even) Higgs sector is given (in the $\overline{\text{MS}}$ scheme and in the Feynman gauge) by [90]

$$\begin{aligned}
V_{\text{eff}} &= V_{\text{tree}} + V_{\text{CW}} \\
&= V_{\text{tree}} + \frac{1}{64\pi^2} \left(\sum_h n_h m_h^4 \left[\ln \left(\frac{m_h^2}{Q^2} \right) - 3/2 \right] + \sum_V n_V m_V^4 \left[\ln \left(\frac{m_V^2}{Q^2} \right) - 5/6 \right] \right. \\
&\quad \left. - \sum_V \frac{1}{3} n_V m_V^4 \left[\ln \left(\frac{m_V^2}{Q^2} \right) - 3/2 \right] - \sum_f n_f m_f^4 \left[\ln \left(\frac{m_f^2}{Q^2} \right) - 3/2 \right] \right),
\end{aligned} \tag{3.1}$$

where V_{tree} is the tree-level potential for the CP -even Higgs fields h_u , h_d and s (see appendix A) and V_{CW} is the well-known Coleman-Weinberg [64] one-loop correction to V_{tree} whose form is shown in the second and the third lines of the equation. There, m_j and n_j are the field-dependent ($\overline{\text{MS}}$) masses (see Appendix C) and the degrees of freedom for the species ‘ j ’, respectively, and the n_j ’s are found to be as follows:

$$\begin{aligned}
n_{h_i^0} = n_{A_i^0} = n_{H_i^+} = n_{H_i^-} &= 1, & n_{W^+} = n_{W^-} = n_Z &= 3, \\
n_t = n_b = 12, n_\tau &= 4, & n_{\chi_i^0} = 2, n_{\chi_1^+} = n_{\chi_1^-} &= 2.
\end{aligned} \tag{3.2}$$

Note that the scalar states, A_i^0 and H_i^\pm , include the Goldstone bosons and that the wino-like states are taken to be decoupled (as pointed out in section 2.2). At finite-temperatures, the

¹In the context of the NMSSM, $\gamma_{\text{EW}} = \frac{\phi_n}{T_n} = \frac{\Delta S U(2)}{T_n} = \frac{\sqrt{((h_d)_{\text{true}} - (h_d)_{\text{false}})^2 + ((h_u)_{\text{true}} - (h_u)_{\text{false}})^2}}{T_n}$.

(CP -even) Higgs-sector potential receives additional contributions that are (in the Feynman gauge) given by [65, 66, 91]

$$\tilde{V}_T = \frac{T^4}{2\pi^2} \left[\sum_h n_h J_B \left(\frac{m_h^2}{T^2} \right) + \sum_V n_V J_B \left(\frac{m_V^2}{T^2} \right) - \sum_V \frac{1}{3} n_V J_B \left(\frac{m_V^2}{T^2} \right) + \sum_f n_f J_F \left(\frac{m_f^2}{T^2} \right) \right], \quad (3.3)$$

where the thermal function J_B (J_F) captures the relevant thermal contribution from the bosons (fermions), and is given by

$$J_{B/F}(y^2) = \pm \text{Re} \int_0^\infty x^2 \ln \left(1 \mp \exp^{-\sqrt{x^2+y^2}} \right) dx, \quad (3.4)$$

with the upper (lower) signs appearing for bosons (fermions). This reveals that for $m_i^2 \gg T^2$, i.e., for large $|y^2|$, these thermal functions are exponentially (Boltzmann-) suppressed. Hence any massive new physics excitation that has been integrated out from the theory could never have a finite-temperature implication. In the reverse limit, i.e., at high temperatures with $|y^2| \ll 1$, $J_{B/F}$ can be approximated as

$$J_B(y^2) \approx J_B^{\text{high-}T}(y^2) = -\frac{\pi^4}{45} + \frac{\pi^2}{12} y^2 - \frac{\pi}{6} y^3 - \frac{1}{32} y^4 \ln \left(\frac{y^2}{a_b} \right), \quad (3.5a)$$

$$J_F(y^2) \approx J_F^{\text{high-}T}(y^2) = -\frac{7\pi^4}{360} + \frac{\pi^2}{24} y^2 + \frac{1}{32} y^4 \ln \left(\frac{y^2}{a_f} \right), \quad (3.5b)$$

where $a_b = \pi^2 \exp(3/2 - 2\gamma_E)$ and $a_f = 16\pi^2 \exp(3/2 - 2\gamma_E)$, γ_E being the Euler-Mascheroni constant (≈ 0.577). The term $-\frac{\pi}{6} y^3$ appearing in the high-temperature expansion of J_B in equation 3.5a gives rise to a negative contribution cubic in the bosonic field in the finite-temperature effective potential \tilde{V}_T . As pointed out earlier, the presence of this term can generate an energy barrier between two degenerate vacua, thus facilitating an SF OPT. Note that such a cubic term appears only for bosonic degrees of freedoms as it comes from the (Matsubara) zero mode propagator which exists only for them.²

At high temperatures, the perturbative approximations at one-loop suffer from large temperature-dependent contributions from additional higher-order processes given by the so-called ‘‘daisy’’ (or ‘‘ring’’) diagrams. Their dominant contributions to the scalar masses obtained from the resummation of these diagrams are captured in the daisy potential given by [93–95]

$$V_{\text{daisy}} = \frac{-T}{12\pi} \left(\sum_h n_h \left[(M_h^2)^{\frac{3}{2}} - (m_h^2)^{\frac{3}{2}} \right] + \sum_V \frac{1}{3} n_V \left[(M_V^2)^{\frac{3}{2}} - (m_V^2)^{\frac{3}{2}} \right] \right), \quad (3.6)$$

where M_h^2 and M_V^2 are the eigenvalues of the thermally improved (i.e., Debye-corrected) mass-squared matrices of the Higgs and the gauge bosons which are presented in Appendix C [93]. Note that only the longitudinal mode of each of the gauge bosons contributes to the daisy potential of equation 3.6. The one-loop finite-temperature effective potential thus becomes

$$V_T = V_{\text{eff}} + \tilde{V}_T + V_{\text{daisy}}, \quad (3.7)$$

²For a discussion in the context of SM, see, for example, reference [92] and the review articles [8, 15, 17, 19, 73]

which is then used in the study of EWPT where one tracks its minima as a function of temperature. Its profile for $T \simeq T_c$ is important for the purpose. However, the locations of the extrema of V_T , as well as the ratio $\phi_c(T_c)/T_c$, are both gauge-dependent [65, 96–100]³ see, for example, references [90, 101–104]. We have checked the minimization of V_T using both Landau and Feynman gauges and have found that the gauge-dependencies of both $\phi_c(T_c)$ and T_c are not significant for the benchmark scenarios we present.

It should be noted here that even for moderately heavy top squarks, which couple intensely to the doublet Higgs fields with the top quark Yukawa coupling, y_t , their presence would give rise to large logarithms in V_{CW} (in equation 3.1) because of a large enough hierarchy between m_t and $m_{\tilde{t}_{1,2}}$. Such large corrections to tree-level potential point to significant dependence of the results on the renormalization scale ‘ Q ’ and a reliable study of phase transition would thus call for treating the potential at higher orders.

To circumvent the problem, one could adopt the effective field theory (EFT) approach in which the top squarks are integrated out from the theory thus resulting in a scenario with two Higgs doublets, a singlet scalar, the electroweakinos and the entire SM spectrum. Thus, the scalar sector of this scenario matches with the one known in the literature [105–107] as the (Z_3 -symmetric) Two Higgs Doublet Model with a Singlet scalar (THDMS) extension of the SM. Hence we adopt the tree-level scalar potential of the THDMS in the present work to study EWPT and make use of the relevant results obtained in references [37, 52, 105–107] where a similar consideration is made. The model parameters of the tree-level scalar potential of the Z_3 -symmetric THDMS are derived in terms of those appearing in the corresponding potential in the Z_3 -NMSSM at the scale M_{SUSY} where the latter is matched onto the former. This correspondence is discussed in Appendix A. We, thus, adopt the following steps [37] to compute the effective potential appropriate for our present study.

- The NMSSM model parameters are taken to be the $\overline{\text{DR}}$ ones at the scale $M_{\text{SUSY}} (= \sqrt{m_{\tilde{Q}_3} m_{\tilde{U}_3}})$ following the convention of the spectrum generator `NMSSMTools` [48] which we use for generating the particle spectrum.
- Following references [37, 52, 105–107], the relevant THDMS parameters appearing in $V_{\text{tree}}^{\text{THDMS}}$ of equation A.2 are then expressed, at the scale M_{SUSY} , in terms of the NMSSM parameters appearing in $V_{\text{tree}}^{\text{NMSSM}}$ of equation A.1 by taking into account the relevant threshold correction that arises as the top squarks are integrated out (see Appendix A).
- We assume that except for the additional Higgs bosons and the higgsino-, the singlino- and the bino-like electroweakinos, all new physics excitations are rather heavy and hence decoupled. Thus, we use the appropriate set of renormalization group equations (RGEs) which now include contributions from all the states in the THDMS scenario, along with those from these lighter electroweakinos, to obtain the respective THDMS parameters at a reference renormalization scale m_t at which the logarithmic contribution from the top quark to the physical minimum of the potential is minimized, and which, also closely resembles the energy scale for the EWSB. V_{tree} (at zero temperature) is then expressed

³The gauge-independent quantities of the effective potential are found using the Nielsen identities [96, 97].

in terms of these parameters of the THDSM at the scale m_t . To make the present work self-contained, we present the set of relevant RGEs [37] in Appendix B.

- We then evaluate the zero-temperature one-loop contribution V_{CW} of equation 3.1. Further, we make use of a specific renormalization condition to ensure the dependence of V_{CW} on the renormalization scale (Q) is minimized [108] (see appendix C). Finally, the finite-temperature effective potential, V_T , for the CP -even scalar fields, are obtained as described earlier.

We have used the package `CosmoTransitions` [55] to track the evolution of the finite-temperature effective potential V_T and to find T_c . Further, the evolution of the potential for $T \lesssim T_c$ has also been studied in order to determine if successful bubble nucleation could occur for our benchmark scenarios. As has been done in some recent studies [52, 54], we also study in detail the patterns of phase transitions for some of these scenarios. These pertain to issues like the number of steps taken for the transition to complete, whether it is of a first or a second-order type and the field directions along which a multi-step transition occurs.

3.2.2 Target region of the NMSSM parameter space

In this section we take a brief overall look into what the possibility of an efficient SFOEWPT would imply for the Z_3 -NMSSM parameter space when experimental constraints, in particular, from the observed Higgs sector and from the DM-sector, are also factored in. This leads to our target region of the parameter space from which we choose a few benchmark scenarios to examine their viability against recently reported LHC results on searches of electroweakinos.

For the purpose, it would be instructive to take a quick look into the tree-level NMSSM potential, $V_{\text{tree}}^{\text{NMSSM}}$, of equation A.1. Considering only the singlet field, a suitable barrier in the potential profile that makes an SFOPT possible develops when the relative contribution from the trilinear term $\sim \kappa A_\kappa s^3$ increases in comparison to the quartic term $\sim \kappa^2 s^4$.⁴ The strength of the transition (parametrized by the ratio of the cubic to the quartic term) increases for a reduced ‘ κ ’ since the latter term diminishes faster. Generically, for a given FOPT, increasing A_κ (i.e., enhancing the cubic term above) strengthens the same. Furthermore, the term trilinear in the singlet and the doublet scalar fields ($\sim \lambda A_\lambda h_d h_u s$) in $V_{\text{tree}}^{\text{NMSSM}}$ could further reinforce the SFOPT (which can now take place in all field directions) for a suitable A_λ . It has also been noted [33, 35] that an SFOEWPT prefers relatively light singlet- and doublet-like scalars.

The upshot is the following. A smaller ‘ κ ’ that an SFOPT already prefers leads to a lighter h_s . At the same time, this causes a singlino-like state to turn lighter which has crucial implications for the DM and the LHC phenomenologies. On the other hand, to find a_s on the lighter side, A_κ needs to be so optimally small that it does not make its contribution to the cubic soft term, $\sim \kappa A_\kappa s^3$, insignificant. A near-parallel argument holds for the requirement on the size of A_λ which controls the masses of the doublet-like Higgs

⁴Such an interplay has been reviewed in the context of the thermally corrected effective scalar potential of the SM [73].

states and has a somewhat similar role to play for the potential profile via the trilinear term $\sim \lambda A_\lambda h_d h_u s$ as does A_κ via the terms cubic in ‘ s ’, as mentioned above.

It may, however, be noted that since h_s could mix with h_{SM} on EWSB, a light h_s quickly attracts stringent bounds from the experimental studies of h_{SM} . Furthermore, a light h_s is also somewhat disfavored by the observed upper limits on the DMDD-SI rates from various DM experiments unless in the presence of a so-called blind spot [109–113] occurring due to a destructive interference among the diagrams with CP -even Higgs states appearing in their propagators. Hence settling for a lone, light a_s with a sizable coupling with h_{SM} is a safer option when looking for an SFOEWPT in the Z_3 -NMSSM. Note, however, that regions of parameter space over which h_{SM} could have on-shell decays to h_s and/or a_s (i.e., when $m_{h_s, a_s} < m_{h_{\text{SM}}}/2$) would be highly constrained by the latest LHC data on h_{SM} [114–117].

As we have discussed earlier, opting for smaller values of ‘ κ ’ would, in turn, result in a light singlino-like LSP ($m_{\tilde{\chi}_1^0} = \sqrt{2}\kappa v_s$) which could be the viable DM candidate of the scenario. Apropos of this, as mentioned earlier, a light higgsino-triplet (comprised of a pair of neutralinos and a chargino) resulting from a smaller $\mu_{\text{eff}} = \lambda v_s/\sqrt{2}$ is very much in the context of the present work which, under circumstances, could as well provide the LSP. A larger value of v_s can re-introduce the problems with large logarithms from one-loop corrections since the field-dependent masses depend on v_s . Keeping this in mind, we consider $v_s \leq 2$ TeV. Thus, relatively small values of μ_{eff} ($\mathcal{O}(100)$ GeV) is achievable for reasonably large values of ‘ λ ’. This, in conjunction with relatively small values of $\tan\beta$ (< 10), helps find $m_{h_{\text{SM}}}$ in the right ballpark, even for not-so-heavy top squarks thus letting $m_{h_{\text{SM}}}$ appear somewhat ‘natural’ [118–121]. We, however, have not restricted ourselves very strictly to this regime and allowed for somewhat larger values of soft masses ($m_{\tilde{Q}_3}$ and $m_{\tilde{U}_3}$) for the squarks and trilinear coupling (A_t) from the third generation.

For smaller values of $\tan\beta$, on the other hand, some extra regions of the parameter space could now find compliance with the DMDD-SI constraints by exploiting the so-called ‘coupling blind spot’ condition $g_{h_{\text{SM}}\chi_1^0\chi_1^0} = 0 \Rightarrow m_{\chi_1^0}/\mu_{\text{eff}} = \pm \sin 2\beta$ (‘+ (–)’) for singlino (bino)-like LSP⁵ when $|\mu_{\text{eff}}|$ tends to approach the LSP mass. This allows us to study a rather nontrivial setup within the NMSSM with a large possible mixing of the higgsinos with the singlino or with the bino. Note that M_1 is not expected to influence the physics of the phase transitions in any drastic way since it enters the calculation of the finite-temperature effective potential via radiative corrections. Hence we have chosen its values (around the electroweak scale) to suit our purpose on DM and collider physics grounds. Thus, an involved situation might arise when all of ‘ κ ’, μ_{eff} and M_1 are on the smaller side such that any of the lighter electroweakinos can be dominantly of a particular type or even mixed states. As we will soon find, its implications for the phenomenology of the electroweakinos at the LHC are rather subtle in connection to the physics of both DM and EWPT. It must, however, be noted that since the DMDD-SD rate has the dependence $\sigma^{\text{SD}} \propto 1/\mu_{\text{eff}}^4$, lowering μ_{eff} beyond a point would quickly attract stringent bounds from the relevant DMDD experiments.

⁵More involved general blind spot conditions of DMDD-SI and -SD cross sections for the 4×4 neutralino (bino-higgsino-singlino) system is derived in [122].

Furthermore, given that we, by now, find that the optimal setup prefers smaller values of $\tan\beta$, we could afford to consider doublet-like heavy Higgs bosons ($'H'$ and $'A'$) of the scenario to be on the lighter side and still passing the latest relevant constraints on them from the LHC experiments in the form of bounds on the $m_{H^\pm}-\tan\beta$ [123] and $m_A-\tan\beta$ [124] planes. This is of some importance since relatively light doublet-like Higgs bosons could potentially render the FOEWPT stronger, provided such a light $'H'$ survives the DMDD-SI constraints. The stage is now set for a brief but important discussion on the phenomenology of such (relatively) light electroweakinos. Dedicated LHC searches for these states over the past years have put stringent lower bounds on their masses and those are becoming even stronger with time. However, these analyses are generally restricted to simplified MSSM scenarios in terms of the spectrum/hierarchy of these states and their consequent patterns of cascades leading to the final states of interest. In general, a scenario like Z_3 -NMSSM could easily invalidate such assumptions in the presence of possible new, light states (for example, the light singlet-like scalars and the singlino). These could then diminish the sensitivities of various target final states and/or tailored signal regions to the experimental analyses thus weakening the lower bounds on the masses of such electroweakinos. In fact, there are myriad such possibilities in our current Z_3 -NMSSM setup which could lead to such a situation [122, 197]. On top of that, the LHC experiments mostly assume (at least, the analyses that are relevant for the present work) the electroweakinos produced in the hard scattering are of wino type for which the relevant cross sections are the largest.

Given the wino decouples from our analysis, for any specific mass the next largest cross section is for the higgsino-pairs which is already about half of that for a corresponding wino-like pair. This further reduces the sensitivity of various final states to the experimental analyses. As has been already pointed out, given the central role that μ_{eff} plays in the DM and EWPT sectors, the search for light higgsino-like states has now become of special significance. The bottom line is that the published lower bound on the electroweakino masses are bound to get more relaxed for these higgsino-like states under a situation different from what the experiments assumed for their analyses. However, it is not a straightforward exercise to come up with the relaxed bounds for a given new situation and any such attempt requires thorough recasts of the existing analyses which we will attempt in this work.

On a conservative note, we do not consider possible situations which could result in weakened bounds on the masses of the electroweakinos when these have a compressed spectrum. In our case, for a light higgsino-triplet with a higgsino-like LSP, the lower bound on μ_{eff} could go down to a value as small as ~ 220 GeV, even with 139 fb^{-1} of data [125, 126].

Guided by the above understanding, we lay down our strategy in section 4 for numerical exploration of the scenario before presenting there our results.

3.3 Production of GW from first-order phase transition

Given that the NMSSM could provide us with an ideal setup for an FOPT that might have taken place in the early Universe, a study of GW originating from such an FOPT, in the context of our present work, is in order. As noted in the Introduction, GW from an FOPT would exist in the form of a stochastic background and has been proposed to be searched for

using the so-called ‘‘cross-correlation’’ method [127–131]. The salient mechanisms via which GW could arise from an FOPT and their corresponding contributions to the GW energy density (scaled by the critical density ρ_c for the Universe with a vanishing cosmological constant Λ) are as follows.

- Collisions of the expanding bubble walls release stress energy located at their walls, as well as lead to possible subsequent shocks, in the intervening plasma made up of relativistic particles [132–137]. However, for a phase transition occurring in a thermal plasma, their contributions to GW energy density are believed to be negligible [138] and hence can be ignored.
- Bulk motion (velocity perturbations) of the plasma generates sound (acoustic) waves (longitudinal modes) that propagate in the same during the time interval between collisions of bubbles and the expanding new phases dissipating their kinetic energy in the plasma [139–142]. These sound waves contribute to the GW energy density as $\Omega_{\text{sw}}h^2$, where $h = H_0/(100 \text{ km} \cdot \text{sec}^{-1} \cdot \text{Mpc}^{-1}) \approx 0.674$ [143], with H_0 standing for the present-day (red-shift $z = 0$) value of the Hubble parameter, also known as the Hubble constant. Such acoustic contributions, when accumulated over the said duration, are expected to dominate.
- Turbulence in the plasma of magneto-hydrodynamic (MHD) origin set up on collisions of the bubbles [144–149] contributes to GW energy density as $\Omega_{\text{turb}}h^2$.

The overall GW energy density can be approximated as a linear combination of the latter two contributions, i.e.,

$$\Omega_{\text{GW}}h^2 \simeq \Omega_{\text{sw}}h^2 + \Omega_{\text{turb}}h^2. \quad (3.8)$$

A few key FOPT parameters, in addition to the bubble nucleation temperature, T_n , that can be obtained from the particle physics models and which control these two contributions can be categorized as follows.

- The parameter ‘ α ’, which relates to the energy budget of the FOPT, is given by [150]

$$\alpha = \frac{\rho_{\text{vac}}}{\rho_{\text{rad}}^*} = \frac{1}{\rho_{\text{rad}}^*} \left[T \frac{\partial \Delta V(T)}{\partial T} - \Delta V(T) \right] \Bigg|_{T_*}, \quad (3.9)$$

where $T_* = T|_{t_*}$ with t_* being the instant of time when the FOPT completes. In the absence of significant effects from reheating, $T_* \simeq T_n$. $\Delta V(T) = V_{\text{low}}(T) - V_{\text{high}}(T)$ is the difference between the potential energies at the false and the true minima and $\rho_{\text{rad}}^* = g_*\pi^2 T^4/30$ where g_* is the number of the relativistic degrees of freedom at $T = T_*$, taken here to be ~ 100 , following recent literature.

- The parameter ‘ β ’, which gives the inverse time-duration of the FOPT, can be derived in terms of the effective 3-dimensional Euclidean action ($S_3(T)/T$) as [135]

$$\beta = - \frac{dS_3(T)}{dt} \Bigg|_{t_*} \simeq H_* T_* \frac{d(S_3(T)/T)}{dT} \Bigg|_{T_*}, \quad (3.10)$$

where $H_* = H|_{T_*}$. For a stronger GW signal, the EWPT should occur over a larger duration of time, i.e., it should be a slow process and hence the ratio β/H_* needs to be on the smaller side.

- The parameter v_w , which pertains to the bubble dynamics, i.e., the wall-velocity of the expanding bubble, needs to be larger for a more intense GW emission, although an optimally strong EWBG is known to be favored only for a tiny, subsonic v_w instead.

The sound wave contribution to the GW energy density, $\Omega_{\text{sw}}h^2$, as a function of the above FOPT parameters and the frequency ‘ f ’ of the GW, is then given by [139, 151, 152]

$$\Omega_{\text{sw}}h^2 = 2.65 \times 10^{-6} \Upsilon(\tau_{\text{sw}}) \left(\frac{\beta}{H_*}\right)^{-1} v_w \left(\frac{\kappa_v \alpha}{1 + \alpha}\right)^2 \left(\frac{g_*}{100}\right)^{-\frac{1}{3}} \left(\frac{f}{f_{\text{sw}}}\right)^3 \left[\frac{7}{4 + 3\left(\frac{f}{f_{\text{sw}}}\right)^2}\right]^{\frac{7}{2}}, \quad (3.11)$$

where κ_v is the fraction of the energy from the phase transition that gets converted into the bulk motion of the plasma which leads to GW and is of the form [63, 153]

$$\kappa_v \simeq \left[\frac{\alpha}{0.73 + 0.083\sqrt{\alpha} + \alpha}\right], \quad (3.12)$$

f_{sw} is the present day peak frequency for the sound wave contribution to GW energy density given by (with the approximation $T_* \approx T_n$) [137]

$$f_{\text{sw}} = 1.9 \times 10^{-5} \text{ Hz} \left(\frac{1}{v_w}\right) \left(\frac{\beta}{H_*}\right) \left(\frac{T_n}{100 \text{ GeV}}\right) \left(\frac{g_*}{100}\right)^{\frac{1}{6}}, \quad (3.13)$$

$\Upsilon(\tau_{\text{sw}})$ is the parameter that brings in the effect of a finite lifetime of the sound waves which suppresses their contributions to the GW energy density and is given by [154, 155]

$$\Upsilon(\tau_{\text{sw}}) = 1 - \frac{1}{\sqrt{1 + 2\tau_{\text{sw}}H_*}}, \quad (3.14)$$

where the lifetime τ_{sw} is considered as the time scale when the turbulence develops and is given by $\tau_{\text{sw}} \approx R_*/\bar{U}_f$ [152, 156], where, in turn, $R_* = (8\pi)^{1/3}v_w/\beta$ is the mean bubble separation [154, 157] and $\bar{U}_f = \sqrt{3\kappa_v\alpha/4}$ is the root-mean-squared (RMS) fluid velocity obtained from a hydrodynamic analysis [60, 157]. Note that as $\tau_{\text{sw}} \rightarrow \infty$, $\Upsilon \rightarrow 1$, asymptotically. On the other hand, for all our benchmark scenarios presented in section 4.3.2, $\tau_{\text{sw}}H_* < 0.1$ when $\Upsilon \rightarrow \tau_{\text{sw}}H_*$. Furthermore, there is a growing realization [158] that v_w might not enter the calculation of the EWBG. Then, to maximize the strength of the GW, it is assumed that the expanding bubbles attain a relativistic terminal velocity in the plasma, i.e., we consider $v_w \simeq 1$.

Similarly, the MHD turbulence contribution to the GW energy density is given by [127]

$$\Omega_{\text{turb}}h^2 = 3.35 \times 10^{-4} \left(\frac{\beta}{H_*}\right)^{-1} \left(\frac{\kappa_{\text{turb}}\alpha}{1 + \alpha}\right)^{\frac{3}{2}} \left(\frac{100}{g_*}\right)^{\frac{1}{3}} v_w \frac{(f/f_{\text{turb}})^3}{[1 + (f/f_{\text{turb}})]^{\frac{11}{3}}(1 + 8\pi f/h_*)}, \quad (3.15)$$

λ	$ \kappa $	$\tan\beta$	$ \mu_{\text{eff}} $ (GeV)	$ A_\lambda $ (TeV)	$ A_\kappa $ (GeV)	$ M_1 $ (GeV)	$ A_t $ (TeV)	$m_{\tilde{Q}_3}$ (TeV)	$m_{\tilde{U}_3}$ (TeV)
0.2–0.7	≤ 0.5	1–20	≤ 500	≤ 2	≤ 200	≤ 500	≤ 5	2–5	2–5

Table 1. Ranges of various model parameters adopted for scanning the Z_3 -NMSSM parameter space. The fixed values of various soft parameters used are as follows: $m_{\tilde{D}_3} = m_{\tilde{L},\tilde{E}} = 3.5$ TeV, $A_{b,\tau} = 3$ TeV, $M_3 = 3$ TeV and $M_2 = 2.5$ TeV.

where k_{turb} is not precisely known but is expected to be in the range of 5%–10% of k_v [142]. We set $k_{\text{turb}} = 0.1k_v$ in our calculation. The present-day peak frequency f_{turb} of the GW spectrum from the turbulence contribution is given by

$$f_{\text{turb}} = 2.7 \times 10^{-5} \text{ Hz} \frac{1}{v_w} \left(\frac{\beta}{H_*} \right) \left(\frac{T_*}{100 \text{ GeV}} \right) \left(\frac{g_*}{100} \right)^{\frac{1}{6}}, \quad (3.16)$$

with $h_* = 16.5 \times 10^{-6} \text{ Hz} \left(\frac{T_n}{100 \text{ GeV}} \right) \left(\frac{g_*}{100} \right)^{\frac{1}{6}}$.

4 Results

In this section we start by presenting the ranges of various input parameters of the scenario that we adopt to carry out a scan over the theory space. This is followed by a brief discussion on the pertinent constraints coming from relevant DM and collider experiments including the crucial ones arising from the studies of the observed Higgs boson to which we subject the scan. A few benchmark scenarios are then chosen for which SFOEWPT occurs. To pursue the central goal of this work, these scenarios are further classified to show how, in the light of what we discuss in section 3.2.2, a few of them with relatively small μ_{eff} get disallowed by current LHC searches for the electroweakinos while some others survive. The prospects of finding GW signals at future experiments are briefly discussed for these surviving scenarios.

In table 1 we present the ranges of the input parameters that we scan over and mention the values of the relevant ones which are kept fixed. The choices are broadly motivated by the discussion in section 3.2.2.

4.1 Constraints from various sectors

In this work, we take into account constraints from various sectors, both theoretical and experimental. The theoretical ones include ensuring the spectra to be free from tachyonic states, the scalar potential not develop an unphysical global minimum and the evolutions of various pertinent couplings of the theory with energy not encounter Landau poles, etc. The experimental constraints include those coming from the Higgs, the DM and the flavor sectors and from various searches for new physics at the colliders. We further ensure the occurrence of SFOEWPT that facilitates EWBG and that such a transition does end up in the physical vacuum. To impose these constraints and for our general numerical analysis, we employ publicly available packages like `NMSSMTools` (v5.5.3) [159, 160], `HiggsBounds` (v5.8.0) [161],

`HiggsSignals` (v2.5.0) [162], `CheckMATE` (v2.0.34) [163], `SModelS` (v2.1.1) [164] and `CosmoTransitions`(v2.0.6) [55]. Below we briefly point out some of the important constraints that are obtained from these packages.

- `NMSSMTools` is used to compute and constrain various relevant observables from the Higgs, the DM, the flavor and the collider sectors. We impose the 2σ upper limit on the DM relic abundance, i.e., $\Omega h^2 \leq 0.131$ as reported by the Planck experiment [4, 181]. The most recent (and improved) upper bounds on the DMDD-SI [182] and -SD [183, 184] rates are taken into account after a commensurate downward scaling of these cross-sections (as the relic abundance drops below the Planck-allowed band) is done. This helps the computed DMDD-SI and -SD rates comply with the respective stringent upper bounds. For all the above-mentioned DM observables, their values are obtained from a dedicated package like `micrOMEGAs` (v4.3) [185] as adapted in `NMSSMTools`. The latter also takes into account, albeit simplistically, the constraints from the CMS analysis on the electroweakino searches in the $3\ell + \cancel{E}_T$ final state with 35.9 fb^{-1} worth of data [165].
- Using `HiggsBounds` and `HiggsSignals`, we retain only those parameter points which pass the thorough checks of the Higgs sector. With the help of the latter package, we allow for Higgs signal-strengths which are consistent with the experimental findings at a 2σ level. To take into account the theoretical uncertainties in the computation of $m_{h_{\text{SM}}}$, we consider $m_{h_{\text{SM}}}$ over the range $122 \text{ GeV} < m_{h_{\text{SM}}} < 128 \text{ GeV}$.
- A few representative (benchmark) scenarios out of the resulting set are then subjected to thorough recasts, via the packages `CheckMATE` and `SModelS`, of a multitude of relevant LHC analyses that include several recent ones with 139 fb^{-1} of data. These analyses and their availabilities in these two packages are indicated in table 2. Together, these are expected to provide us with the most stringent lower bounds on the masses of the electroweakinos under diverse circumstances which are pointed out while discussing those. In addition, there are a few more rather recent LHC analyses [125, 186, 187] which are expected to be sensitive to the scenarios we study but yet not available in the public versions of either of these two packages. We will get back to these in section 4.3.2.
- Parameter points that pass the previous set of constraints are subjected to analyses via `CosmoTransitions` to check for SFOEWPT that results in the physical EW vacuum.

We, however, do not consider the recent experimental finding on muon $(g-2)$ [188, 189] since the dust is yet to settle over its BSM implications. We, thus, have set the masses of the smuons, along with all the sfermions, at a multi-TeV range.

When using `CheckMATE`, we have generated, for each such analysis, Monte Carlo events for the leading order productions of all pertinent pair and associated productions of various electroweakinos at the 13 TeV LHC, i.e., for $pp \rightarrow \chi_j \chi_k$, ($\chi_{j,k} \in \{\chi_i^0, \chi_1^\pm\}$, with $i \in \{1-4\}$), with up to two additional partons, using `MadGraph5` [190]. These events are then passed through `PYTHIA8` [191] for generating parton showers, hadronization and decays of the unstable particles. The additional partonic jets from the matrix elements are then matched to those

Analysis (Luminosity)	Process	Final State	SModelS	CheckMATE
CMS-SUS-17-004 [165] (35.9 fb ⁻¹)	$\chi_2^0 \chi_1^\pm \rightarrow Z/h_{\text{SM}} \chi_1^0 W^\pm \chi_1^0$	$(m \geq 0)\ell + (n \geq 0)\tau + \cancel{E}_T$		✓
CMS-SUS-16-048 [166] (35.9 fb ⁻¹)	$\tilde{t}\bar{t} \rightarrow b\chi_1^\pm b\chi_1^\mp$ $\chi_2^0 \chi_1^\pm \rightarrow Z^* \chi_1^0 W^{\pm*} \chi_1^0$	$(k \geq 0)\ell + (m \geq 0)b + (n \geq 0)\text{-jet} + \cancel{E}_T$		✓
CMS-SUSY-16-039 [167] (35.9 fb ⁻¹)	$\chi_2^0 \chi_1^\pm \rightarrow \ell\bar{\ell}\tilde{\nu}$ $\chi_2^0 \chi_1^\pm \rightarrow \ell\bar{\ell}\tilde{\tau}\nu$ $\chi_2^0 \chi_1^\pm \rightarrow \tilde{\tau}\tau\tilde{\nu}$ $\chi_2^0 \chi_1^\pm \rightarrow Z\chi_1^0 W^\pm \chi_1^0$ $\chi_2^0 \chi_1^\pm \rightarrow h_{\text{SM}}\chi_1^0 W^\pm \chi_1^0$	$(n \geq 0)\ell + \cancel{E}_T$	✓	✓
CMS-SUS-17-010 [168] (35.9 fb ⁻¹)	$\chi_1^\pm \chi_1^\mp \rightarrow W^\pm \chi_1^0 W^\mp \chi_1^0$ $\chi_1^\pm \chi_1^\mp \rightarrow \nu\bar{\ell}\ell\bar{\nu}$	$2\ell + \cancel{E}_T$	✓	
CMS-SUS-16-043 [169] (35.9 fb ⁻¹)	$\chi_2^0 \chi_1^\pm \rightarrow h_{\text{SM}}\chi_1^0 W^\pm \chi_1^0$	$1\ell + 2b + \cancel{E}_T$	✓	
CMS-SUS-16-045 [170] (35.9 fb ⁻¹)	$\chi_2^0 \chi_1^\pm \rightarrow h_{\text{SM}}\chi_1^0 W^\pm \chi_1^0$	$1\ell + 2\gamma + \cancel{E}_T$	✓	
CMS-SUS-16-034 [171] (35.9 fb ⁻¹)	$\chi_2^0 \chi_1^\pm \rightarrow Z/h_{\text{SM}}\tilde{\chi}_1^0 W^\pm \chi_1^0$	$(m \geq 2)\ell + (n \geq 1)\text{-jet} + \cancel{E}_T$	✓	
ATLAS-1712-08119 [172] (36.1 fb ⁻¹)	$\tilde{\ell}\bar{\ell}$ $\chi_2^0 \chi_1^\pm \rightarrow Z^* \chi_1^0 W^* \chi_1^0$	$2\ell + (n \geq 0)\text{-jet} + \cancel{E}_T$		✓
ATLAS-1803-02762 [173] (35.9 fb ⁻¹)	$\chi_2^0 \chi_1^\pm \rightarrow Z\chi_1^0 W^\pm \chi_1^0$ $\chi_2^0 \chi_1^\pm \rightarrow \nu\bar{\ell}\bar{\ell}$ $\chi_1^\pm \chi_1^\mp \rightarrow \nu\bar{\ell}\nu\bar{\ell}$	$(n \geq 2)\ell + \cancel{E}_T$	✓	✓
ATLAS-1812-09432 [174] (36.1 fb ⁻¹)	$\chi_2^0 \chi_1^\pm \rightarrow h_{\text{SM}}\chi_1^0 W^\pm \chi_1^0$	$(j \geq 0)\ell + (k \geq 0)\text{-jet} + (m \geq 0)b + (n \geq 0)\gamma + \cancel{E}_T$	✓	
ATLAS-1806-02293 [175] (36.1 fb ⁻¹)	$\chi_2^0 \chi_1^\pm \rightarrow Z\chi_1^0 W^\pm \chi_1^0$	$(m \geq 2)\ell + (n \geq 0)\text{-jet} + \cancel{E}_T$	✓	
ATLAS-1909-09226 [176] (139 fb ⁻¹)	$\chi_2^0 \chi_1^\pm \rightarrow h_{\text{SM}}\chi_1^0 W^\pm \chi_1^0$	$1\ell + 2b + \cancel{E}_T$	✓	
ATLAS-1912-08479 [177] (139 fb ⁻¹)	$\chi_2^0 \chi_1^\pm \rightarrow Z(\rightarrow \ell\ell)\tilde{\chi}_1^0 W(\rightarrow \ell\nu)\tilde{\chi}_1^0$	$3\ell + \cancel{E}_T$	✓	✓
ATLAS-1908-08215 [178] (139 fb ⁻¹)	$\tilde{\ell}\bar{\ell}$ $\chi_1^\pm \chi_1^\mp (\chi_1^\pm \rightarrow W^\pm \chi_1^0)$ $(\chi_1^\pm \rightarrow \tilde{\ell}\nu/\bar{\nu}\ell)$	$2\ell + \cancel{E}_T$	✓	✓
ATLAS-1911-12606 [179] (139 fb ⁻¹)	$\tilde{\ell}\bar{\ell}$ $\chi_1^\pm \chi_2^0 \rightarrow W^*(\rightarrow qq)\chi_1^0 Z^*(\rightarrow ll)\chi_1^0$	$\text{jets} + 2\ell + \cancel{E}_T$		✓
ATLAS-2004-10894 [180] (139 fb ⁻¹)	$\chi_2^0 \chi_1^\pm \rightarrow h_{\text{SM}}(\rightarrow \gamma\gamma)\chi_1^0 W(\rightarrow \ell\nu)\chi_1^0$	$1\ell + 2\gamma + \cancel{E}_T$	✓	✓

Table 2. Relevant experimental analyses, along with the processes and final states considered, in search for the electroweakinos at the 13 TeV LHC with the data sets at $\sim 36 \text{ fb}^{-1}$ and 139 fb^{-1} that are implemented in CheckMATE and/or SModelS.

from the parton showers (the so-called ME-PS matching) using the MLM prescription [192] built-in in `MadGraph5`. The resulting events are passed through `DELPHES` [193] to include the detector effects. For an analysis using `SModelS`, we just provide the package with the SLHA file along with the `MadGraph5`-generated cross sections of various production processes as mentioned earlier. To account for the significant NLO+NLL contributions, all production cross sections have been multiplied by a flat k -factor of 1.25 [194]. Both the recast packages calculate a r -value for a given theory point, where $r = (S - 1.64\Delta S)/S95$, with ‘ S ’, ΔS and $S95$ signifying the predicted number of signal events, the associated Monte Carlo error and the experimental limit on ‘ S ’ at 95% confidence level, respectively. Nominally, $r < (>)1$ indicates the scenario to be allowed (disallowed).

4.2 Choice and study of benchmark scenarios

As pointed out earlier, we now look for a few benchmark scenarios from those that pass the selections of `NMSSMTools`, `HiggsBounds` and `HiggsSignals`. In figure 1 we present scatter plots of parameter points that pass those selections in the plane of $|\mu_{\text{eff}}| - m_{\chi_1^0}$. The choice of the said plane is motivated by the physics of the relatively light electroweakinos that are in the context given the recent LHC searches and from the viewpoint of SFOEWPT. Presenting the bino (left plot) and the singlino (right plot) contents of the LSP (in the palettes) further clarifies the situations from the involved angles.

In both plots, scenarios having a higgsino-dominated LSP arise, by construct, along the diagonals ($m_{\chi_1^0} \approx \mu_{\text{eff}}$). Points along the two horizontal streaks appearing at low $m_{\chi_1^0}$ correspond to a bino- or a singlino-dominated LSP DM that find h_{SM} and Z -boson as funnels in their mutual annihilation. The sparse occurrence of a singlino-dominated LSP over these streaks points to some amount of tuning that is needed among the NMSSM parameters to comply simultaneously with the constraints from the Higgs and the DM sectors, an issue which is not of much concern for a bino-dominated LSP since M_1 could be altered practically freely without affecting the Higgs sector. $m_{\chi_1^0} \lesssim 30$ GeV is disfavored since as a DM candidate χ_1^0 would require a relatively light Higgs boson (a_S or h_S) below ~ 60 GeV for an efficient (funnel) annihilation which, in turn, attracts severe constraints from the studies on h_{SM} decays. Furthermore, the DMDD constraints are rather severe for such $m_{\chi_1^0}$.

In each of these plots, another densely populated region appears along the edge of the diagonal where efficient coannihilations of the DM with closely lying electroweakinos, backed by favorable mixing among these states, are possible. In the rest of the (less populated) regions, compliance with the upper bound on the DM relic abundance is facilitated mainly by various Higgs boson funnels. Derth of points over the region bounded roughly by $100 \text{ GeV} < m_{\chi_1^0} < 200 \text{ GeV}$ and $100 \text{ GeV} < |\mu_{\text{eff}}| < 250 \text{ GeV}$ is due to the constraints derived from the CMS search for electroweakinos in the final state $3\ell + \cancel{E}_T$ with 35.9 fb^{-1} of data [165]. A similar observation was made in reference [195] which finds further support in subsequent studies [196–198]. A low population of points at higher $|\mu_{\text{eff}}|$ and for intermediate values of $m_{\chi_1^0}$ is mostly since the DM tends to be over-abundant due to its sub-optimal coannihilation rate and/or for a lack of suitable annihilation funnels.

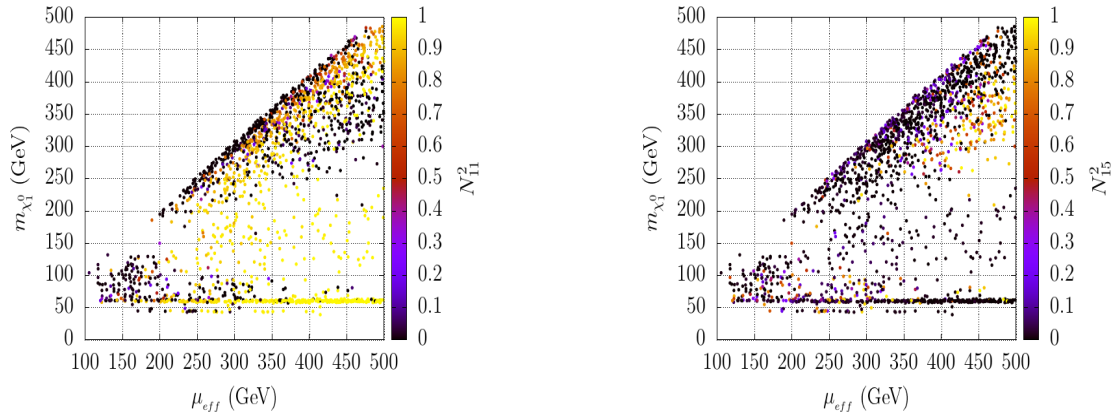


Figure 1. Scatter plots in $\mu_{\text{eff}}-m_{\chi_1^0}$ plane showing points that pass all relevant constraints from `NMSSMTools` (which include various collider and DM constraints), `HiggsBounds` and `HiggsSignals`. Variations of the bino (N_{11}^2 , left) and the singlino (N_{15}^2 , right) contents in the LSP (DM) are indicated via the palettes.

In the subsequent subsections we settle for a few benchmark scenarios out of these allowed set which are representative of various situations of interest. We study their properties related to phase transitions at finite temperatures to ensure that an SFOEWPT (i.e., $\gamma_{\text{EW}} \gtrsim 1$) could occur. It is important to note that while relevant LHC analyses with $\sim 36 \text{ fb}^{-1}$ of data would continue to constrain our scenarios, the entire region of the NMSSM parameter space indicated in figure 1 can now be sensitive to some of the recent LHC searches for the electroweakinos with 139 fb^{-1} of data which all are listed in table 2. Hence we subject the benchmark scenarios to these analyses via their recasts using `CheckMATE` and `SModels`. Furthermore, we check the future experimental sensitivity of the GW produced during the time of phase transition for a few of such allowed scenarios.

4.3 Studying the benchmark scenarios

In this subsection, we discuss how searches for the lighter electroweakinos at the LHC could restrict the region of parameter space which otherwise favors SFOEWPT and satisfy all other experimental bounds. The value of μ_{eff} is in direct reference since a small value of the same, while favors SFOEWPT, draws substantial constraint from the above-mentioned searches. Our goal is to first identify the lowest values of μ_{eff} (or, for that matter, the smallest values of the higgsino-like electroweakino masses, except when these form a triplet which contains the lightest of all the electroweakinos) that would be allowed under different circumstances, followed by a discussion of allowed scenarios with optimally light higgsinos. In the process, we highlight the role of different signal regions that play crucial roles.

For a scenario with a decoupled wino, lower bounds on the masses of the lighter electroweakinos to be derived from the LHC experiments would crucially depend on the values of two quantities, μ_{eff} and κ/λ . This is all the more so for a smaller κ (which favors SFOEWPT) that renders the singlino lighter. With μ_{eff} not so large, electroweakinos, with their dominant contents, could exhibit altered hierarchies in their masses which result in contrasting pat-

terns in their cascades. These, depending on their mutual mass-splits, result in their altered sensitivities to different final states and/or signal regions at the LHC experiments.

A smaller M_1 could add further intricacies to the collider phenomenology [122, 196–198] by placing the bino-like neutralino in the vicinity of the light singlino and the higgsinos while aiding compliance with various constraints from the DM sector. We also stick to small values of $\tan\beta$ ($\lesssim 5$) which favors SFOEWPT. As noted earlier, we further consider relatively large values of ‘ λ ’ ($\gtrsim 0.5$) which, in conjunction with small $\tan\beta$ values, aid compliance with the observed value of $m_{h_{\text{SM}}}$ in a more ‘natural’ way. Note that we seek to allow for relatively small values of m_H as well since those are what is preferred by SFOEWPT. For small values of $\tan\beta$ ($1 \lesssim \tan\beta \lesssim 5$) that we would like to restrict ourselves to, stringent lower bounds on $m_{H^\pm, H, A}$ come dominantly from their searches in the tb (for H^\pm) and $\tau\tau$ (for H, A) final states [123, 124]. While in the general scan of the parameter space, these constraints have eliminated some scenarios, the benchmark scenarios that we work with happen to lie outside the constrained regions. However, for the latter, as and when these become sensitive to similar future analyses, the presence of light electroweakinos in the spectrum could help evade those if the Higgs states could also decay to these electroweakinos. In this regard, searches for H^\pm is expected to be of immediate relevance and hence we mention its altered branching fraction to tb final state for our benchmark scenarios.

Also given that the patterns of vacuum transitions get to be rather involved, we adopt the following convention to describe those in the upcoming discussions. The total number of steps involved in a given phase transition process is denoted by the roman numerals (i.e., I, II, etc.) while the type of the phase transition, i.e., whether it is of a first or a second-order kind, is denoted by the arabic numerals (i.e., 1, 2, etc.). On the other hand, for multi-step phase transitions, the various field directions along which the phase transitions occur are indicated by ‘S’, for the singlet direction and ‘D’, for the $SU(2)$ field directions. For example, a direct, i.e., a one-step, FOPT along all three directions is denoted by ‘I(1)’, whereas a two-step FOPTs in which the first transition takes place along the singlet direction and the subsequent one along the $SU(2)$ field directions is labeled as ‘II-S(1)-D(1)’.

4.3.1 Disallowed scenarios with low μ_{eff}

Benchmark points presented in table 3 are chosen with the following considerations. We seek to get an idea of how large a value of μ_{eff} which is still consistent with SFOEWPT but is expected to be ruled out by the electroweakino searches at the LHC. We employ CheckMATE for the purpose by putting all its currently implemented set of LHC analyses in action. In case we find some such benchmark scenarios to be barely allowed, we subject the same further to SModelS (see table 2) in which a host of relevant LHC analyses (with 139 fb^{-1} of data) are incorporated to check if that is still the case.

In BP-D1, the LSP is singlino-dominated with $m_{\tilde{\chi}_1^0} \sim 60 \text{ GeV}$. The higgsino-like electroweakinos are the immediately heavier states with their masses governed by $|\mu_{\text{eff}}|$ ($\sim 275 \text{ GeV}$) and range over $280 \text{ GeV} - 310 \text{ GeV}$. We set $M_1 \sim 480 \text{ GeV}$ such that the bino-dominated neutralino effectively decouples on both collider and cosmology considerations. The DM relic is under-abundant thanks to the presence of the h_{SM} -funnel which, ‘ λ ’ being

large ($=0.68$), is rather efficient. This effectively scales down the reported upper limits of the DMDD-SI and -SD rates (as a function of $m_{\chi_1^0}$) thus aiding compliance of the scenario with these constraints.

The calculation for T_c in BP-D1 suggests the possibility of a direct (type-I(1)) SFOEWPT ($\Delta_{SU(2)}/T_c = 1.14$) from the trivial false minimum at $\{h_d, h_u, h_s\} \equiv \{0, 0, 0\}$ to the broken, true (global) minimum at $\{h_d, h_u, h_s\} \equiv \{25.5, 145.6, -474.4\}$ GeV at $T_c = 129.5$ GeV. Note, however, that this is the only benchmark point that we present for which the phase with the true minimum does not nucleate successfully and hence the system would remain trapped at the metastable false minimum ($\{0, 0, 0\}$). This could render much of the parameter space (that otherwise favors SFOEWPT) cosmologically nonviable [54]. Nonetheless, we retain this point as a benchmark to demonstrate some characteristic collider-aspects, as discussed below, which could be equally instrumental in a scenario that does not have this shortcoming.

A CheckMATE analysis rules out BP-D1 (with $r=1.12$) via a CMS analysis [167] of 35.6 fb^{-1} worth data in the $3\ell + \cancel{E}_T$ final state where an opposite-sign, same-flavor (OS-SF) lepton (e or μ)-pair originates in the decay of an on-shell Z -boson coming from the decay of a heavier neutralino. Such a scenario, with μ_{eff} as small as 275 GeV, would anyway be excluded more convincingly (i.e., with a larger r -value) by the recent LHC analyses in references [125, 186] for the same final state which exploit 139 fb^{-1} of data.

The benchmark point BP-D2 is somewhat similar to that in BP-D1 in terms of the phenomenological features that are relevant for our discussion, i.e, the LSP is still singlino-dominated with a very similar mass as before (≈ 60 GeV), the higgsino-like states are again the next heavier excitations with masses not very different (though on a little higher side) from those in BP-D1. Like BP-D1, BP-D2 also possesses relatively light singlet-like scalars. The DM phenomenologies, in both qualitative and quantitative terms, are rather similar in these two cases.

However, in contrast to that in BP-D1, in BP-D2, it is a two-step phase transition (type-II-S(1)-D(2)) as is suggested by the calculations of T_c . First, a broken phase ($\{0, 0, 539.9\}$ GeV) appears only along the singlet direction at $T_c = 151.5$ GeV with a possibility of a first-order phase transition. This is followed by the appearance of another configuration at $T_c = 112.7$ GeV for which $SU(2)$ is now broken in the true minimum. This triggers the possibility of a second-order phase transition in which the scalar field could move from the evolved false minimum to the said true minimum. On the other hand, the calculation for T_n now suggests that the tunneling process corresponding to $T_c = 151.5$ GeV is so slow that what takes place instead is a strong ($\Delta_{SU(2)}/T_n = 2.2$), one-step first-order transition along all three directions simultaneously (type-I(1)) from the trivial to the physical phase ($\{67.0, 197.8, 774.8\}$ GeV) at $T_n = 96.2$ GeV.

On the collider front, BP-D2 yields somewhat smaller production cross sections for the higgsino-like states than what BP-D1 gives because these states are a little heavier in BP-D1. A CheckMATE analysis indicates that in the CMS analysis in reference [167] that uses 35.9 fb^{-1} of data, the same final state ($3\ell + \cancel{E}_T$) with an identical signal region as in BP-D1 becomes the most sensitive of the searches while, this time, barely disallowing ($r = 1.01$) the parameter point. A subsequent SModelS study indicates that the analyses in references [176–

Inputs/Observables	BP-D1	BP-D2	BP-D3
λ, κ	0.683, 0.060	0.547, 0.044	0.565, 0.071
A_λ, A_κ (GeV)	-1352.3, 134.5	978.4, -110.0	963.5, -112.5
μ_{eff} (GeV)	-274.4	308.0	308.0
$\tan\beta$	4.77	2.87	2.87
M_1 (GeV)	478.8	460.3	-57.2
$m_{\tilde{Q}_3}, m_{\tilde{U}_3}$ (GeV)	2956.7, 3378.3	3710.8, 3562.8	3710.8, 3562.8
A_t (GeV)	-1019.7	2204.0	2204.0
$m_{\chi_{1,2,3,4}^0}$ (GeV)	60.9, -304.3, 307.9, 479.4	60.6, 312.7, -338.3, 468.1	-59.6, 91.1, 327.2, -338.4
$m_{\chi_{1,2,3,4}^\pm}$ (GeV)	-284.1	316.3	316.0
$m_{h_1}, m_{h_2}, m_{a_1}$ (GeV)	79.2, 124.4, 126.6	78.1, 122.2, 109.5	86.9, 123.0, 142.6
m_{H^\pm} (GeV)	1359.0	963.8	963.6
$N_{11}, N_{21}, N_{31}, N_{41}$	-0.03, 0.04, -0.13, 0.99	0.03, -0.25, -0.02, 0.97	0.99, -0.07, -0.1, 0.06
$N_{13}, N_{23}, N_{33}, N_{43}$	0.01, -0.71, 0.70, 0.06	-0.04, 0.70, 0.70, -0.16	0.11, -0.03, 0.71, -0.70
$N_{14}, N_{24}, N_{34}, N_{44}$	0.38, 0.65, 0.65, 0.12	-0.27, -0.65, 0.68, 0.19	-0.04, -0.27, -0.68, -0.68
$N_{15}, N_{25}, N_{35}, N_{45}$	0.93, -0.26, -0.27, -0.02	0.96, -0.16, 0.22, 0.02	0.07, -0.96, -0.18, -0.21
$\text{BR}(\chi_{1,2,3,4}^\pm \rightarrow \chi_{1,2,3,4}^0 W^\pm)$	1.00	1.00	0.19
$\text{BR}(\chi_{1,2,3,4}^\pm \rightarrow \chi_{1,2,3,4}^0 Z)$	0.00	0.00	0.81
$\text{BR}(\chi_{1,2,3,4}^0 \rightarrow \chi_{1,2,3,4}^\pm W^\mp)$	0.52	0.58	off-shell
$\text{BR}(\chi_{1,2,3,4}^0 \rightarrow \chi_{1,2,3,4}^0 h_2)$	0.37	0.33	off-shell
$\text{BR}(\chi_{1,2,3,4}^0 \rightarrow \chi_{1,2,3,4}^0 \gamma)$	0.00	0.00	0.15
$\text{BR}(\chi_{1,2,3,4}^0 \rightarrow \chi_{1,2,3,4}^0 Z)$	0.43	0.36	0.03
$\text{BR}(\chi_{1,2,3,4}^0 \rightarrow \chi_{1,2,3,4}^0 h_2)$	0.00	0.00	0.53
$\text{BR}(\chi_{1,2,3,4}^0 \rightarrow \chi_{1,2,3,4}^0 h_1)$	0.34	0.42	0.10
$\text{BR}(\chi_{1,2,3,4}^0 \rightarrow \chi_{1,2,3,4}^0 a_1)$	0.00	0.00	0.27
$\text{BR}(\chi_{1,2,3,4}^0 \rightarrow \chi_{1,2,3,4}^0 a_2)$	0.19	0.16	0.01
$\text{BR}(\chi_{1,2,3,4}^0 \rightarrow \chi_{1,2,3,4}^0 Z)$	0.16	0.12	0.18
$\text{BR}(\chi_{1,2,3,4}^0 \rightarrow \chi_{1,2,3,4}^0 h_2)$	0.12	~ 0	0.31
$\text{BR}(\chi_{1,2,3,4}^0 \rightarrow \chi_{1,2,3,4}^0 h_1)$	0.02	0.09	0.00
$\text{BR}(\chi_{1,2,3,4}^0 \rightarrow \chi_{1,2,3,4}^0 a_1)$	0.00	0.11	0.02
$\text{BR}(\chi_{1,2,3,4}^0 \rightarrow \chi_{1,2,3,4}^0 a_2)$	0.01	~ 0	0.02
$\text{BR}(\chi_{1,2,3,4}^0 \rightarrow \chi_{1,2,3,4}^0 h_2)$	0.01	0.21	0.30
$\text{BR}(\chi_{1,2,3,4}^0 \rightarrow \chi_{1,2,3,4}^0 a_1)$	0.01	~ 0	0.15
$\text{BR}(\chi_{1,2,3,4}^0 \rightarrow \chi_{1,2,3,4}^\pm W^\mp)$	0.48	0.46	0.00
$\text{BR}(H^\pm \rightarrow t\bar{b})$	0.12	0.39	0.37
Ωh^2	4.9×10^{-4}	4.4×10^{-4}	4.8×10^{-3}
$\sigma_{\chi_{1,2,3,4}^0-p(n)}^{\text{SI}} \times \xi$ (cm ²)	$4.5(4.6) \times 10^{-47}$	$2.4(2.5) \times 10^{-47}$	$2.5(2.6) \times 10^{-47}$
$\sigma_{\chi_{1,2,3,4}^0-p(n)}^{\text{SD}} \times \xi$ (cm ²)	$3.5(3.2) \times 10^{-42}$	$7.6(5.8) \times 10^{-43}$	$1.9(1.5) \times 10^{-43}$
First T_c (GeV) / Transition type	129.4 / 1st-order	151.5 / 1st-order	165.7 / 1st-order
$\{h_d, h_u, s\}_{\text{false.vac.}}$ (GeV)	{0, 0, 0}	{0, 0, 0}	{0, 0, 0}
$\{h_d, h_u, s\}_{\text{true.vac.}}$ (GeV)	{25.5, 145.6, -474.4}	{0, 0, 539.9}	{0, 0, 557.5.9}
Second T_c (GeV) / Transition type	-	112.7 / 2nd-order	105.6 / 1st-order
$\{h_d, h_u, s\}_{\text{false.vac.}}$ (GeV)	-	{0, 0, 661.7}	{0, 0, 662.3}
$\{h_d, h_u, s\}_{\text{true.vac.}}$ (GeV)	-	{9.5, 31.5, 668.2}	{12.8, 41.6, 669.0}
T_n (GeV) / (Nucleation) Transition type	-	96.2 / 1st-order	55.9 / 1st-order
$\{h_d, h_u, s\}_{\text{false.vac.}}$ (GeV)	-	{0, 0, 0}	{0, 0, 0}
$\{h_d, h_u, s\}_{\text{true.vac.}}$ (GeV)	-	{67.0, 197.8, 774.8}	{68.1, 199.2, 759.2}
$\gamma_{\text{EW}} = \Delta_{SU(2)}/T_n$	-	2.2	3.8
CheckMATE result	Excluded	Excluded	Excluded
r -value	1.12	1.01	2.13
Analysis ID	CMS.SUS.16.039 [167]	CMS.SUS.16.039 [167]	CMS.SUS.16.039 [167]
Signal region ID	SR_A30	SR_A30	SR_G05

Table 3. Benchmark scenarios allowed by all relevant theoretical and experimental constraints (see text for details) except for those from the LHC searches for the electroweakinos. Shown are the various relevant masses, mixings, branching fractions along with the values of DM observables and details of the EWPT. The most sensitive LHC signal regions that rule out these scenarios, along with the LHC analyses they belong to, are also presented. Other fixed parameters are as indicated in the caption of table 1. The parameter $\xi (= \frac{\Omega h^2}{0.1187})$ is used to scale (down) the DD rates.

178], all involving 139 fb^{-1} of data, are even less sensitive. As for BP-D1, BP-D2 is also likely to be ruled out convincingly by the analyses of $3\ell + \cancel{E}_T$ final state with 139 fb^{-1} of data presented in references [125, 186]. The resulting r -values would hint at how big a μ_{eff} could thus be excluded in such a setup.

The point BP-D3 contains a somewhat heavier ($\sim 91 \text{ GeV}$) singlino-like neutralino state where SFOEWPT ($\Delta_{SU(2)}/T_n = 3.8$) remains viable, ‘ κ ’ being still small (~ 0.071). The relic for such a singlino as a DM candidate is bound to be over-abundant in the absence of a suitable funnel, as is the case with BP-D3. The possibility of an efficient coannihilation, say with a bino-like state, requires a small mass-split between them which then tends to make the DD rates way too large to be acceptable. Instead, a bino-like LSP having a smaller mass and possessing a suitable annihilation funnel via Z - or h_{SM} could qualify as a DM. This is what we find in BP-D3 (with an h_{SM} funnel, with $|m_{\chi_1^0}| \approx 60 \text{ GeV}$). Spectrum-wise, this constitutes its basic difference from BP-D2. The pattern of phase-transition in BP-D3, as obtained from the critical temperature calculation, is also of a two-step kind (type-II-S(1)-D(1)) but is slightly different from what occurs in BP-D2, as can be seen in table 3. Although the bubble nucleation calculation indicates that both benchmark points have one-step SFOPTs in all three directions (type-I(1)).

However, the hierarchy among the lighter neutralinos now triggers important effects with major implications for the searches of the electroweakinos at the LHC. The higgsino-like states predominantly decay to the singlino-like NLSP and the Z -boson and/or h_{SM} thanks to an enhanced higgsino-singlino mixing for a value of ‘ λ ’ which is on the larger side (~ 0.57) [122]. Subsequently, the NLSP neutralino would undergo dominant decays to off-shell Z -boson or h_{SM} . Such cascades result in strengthened multi-lepton (more than three leptons) final states which now become far more sensitive to the recent LHC analyses when compared to the trilepton final states. The reason behind this is a much suppressed SM background for the former [167]. Indeed, a dedicated **CheckMATE** analysis confirms this effect and rules out BP-D3 rather emphatically ($r = 2.13$) by getting sensitive to the right (dedicated for final states with more than 3 leptons) signal region (“G05”) of the CMS analysis in reference [167] which considers data worth 35.9 fb^{-1} only. This needs to be contrasted with the verdict on higgsinos of very similar masses in BP-D2 in which those masses appear to be barely disallowed ($r = 1.01$) with the same set of data. Further, given the heightened sensitivity of the analysis to the multi-lepton final states, it could eventually rule out even heavier higgsino-like states in such a setup.

The exercise undertaken in this section indicates how different types of spectrum for the light higgsino-like electroweakinos (i.e., smaller μ_{eff}), which otherwise comply with all relevant bounds including those from the DM sector and which allow for SFOEWPT, get ruled out by the LHC analyses with $\sim 36 \text{ fb}^{-1}$ of data even when the latter’s sensitivities to the targeted final states deteriorate significantly. The benchmark scenarios are so chosen that we end up with $r \gtrsim 1$. Such a value nominally reflects how light such electroweakinos could get before they start attracting bounds from the LHC analyses. Of course, more recent LHC analyses [125, 186] with 139 fb^{-1} of data are expected to push these mass-bounds (and hence μ_{eff}) upwards but these are yet to be implemented in a recast package.

4.3.2 Allowed benchmark scenarios with successful nucleation

In this section we present a few benchmark scenarios that have all the good qualities of those listed in table 3 but now also pass the lower bounds on the electroweakino masses coming from some of the recent LHC analyses. Naively, this pushes μ_{eff} up which impedes an efficient SFOEWPT with successful nucleation. The SFOEWPT now tends to proceed in two steps the details of which are presented in table 5 for our benchmark points. This is somewhat typical when the trivial and the global minima have a large separation between them in the field space [54]. This is since a larger μ_{eff} corresponds to a larger v_s at zero temperature for a given λ , a feature that governs the field-separation at T_c .

The benchmark points in table 4 are picked up keeping in mind the following issues. While our goal is to find compatible points with smaller values of μ_{eff} , we like to see the resulting scenarios have LSPs with different dominant admixtures. Allowing for this has a considerable bearing on both the DM phenomenology and searches for the electroweakinos at the LHC. Furthermore, these benchmarks possess a light singlet-like scalar below 100 GeV. This is since we set both ‘ κ ’ and A_κ small which is preferred by SFOEWPT. Note that such a light singlet state inevitably affects both DM and collider phenomenologies, more so since the nature of the lighter electroweakinos, including the LSP, could get altered, simultaneously. As has been noted in section 3.2.2, to facilitate SFOEWPT we look for relatively light doublet-like Higgs bosons (by choosing A_λ suitably) which are still allowed by the LHC Higgs searches.

In BP-A1 we have a higgsino-like lightest triplet with masses in the range $\sim 400 - 430$ GeV with $\mu_{\text{eff}} \sim 422$ GeV. Thus, the LSP and the NLSP are both higgsino-like (with their higgsino contents at 70% and 98%, respectively) while the lighter chargino is a nearly pure higgsino. As far as the DM sector is concerned, such a higgsino-like LSP DM is naturally under-abundant ($\Omega h^2 = 3.78 \times 10^{-4}$). This, in turn, generically helps satisfy the DMDD-SI and -SD constraints via downward scaling of the respective cross-sections.

As for the pattern of EWPT in BP-A1, the calculation for T_c suggests that this is a two-step process of the type II-S(1)-D(1) as indicated in table 5 where first, at $T_c = 946.7$ GeV, a broken phase appears in the singlet-direction followed by another in the $SU(2)$ field directions at $T_c = 91.1$ GeV. Subsequently, successful nucleations take place closely below the respective T_c ’s, down at $T_n = 946.6$ GeV and 90.2 GeV. Note that in this particular case, calculations for both T_c and T_n suggest that the first phase transition (in the singlet-only direction) is just of a first-order kind while the second one, in the all-important $SU(2)$ field directions that breaks the electroweak symmetry, is of a ‘strong’ first-order type ($\gamma_{EW} = 1.1$) which is a crucial requirement for EWBG.

Searches for the lighter electroweakinos in BP-A1 effectively amounts to those for the higgsinos only where these states appear as the lightest triplet of electroweakinos which includes the LSP. This is since the heavier neutralinos, χ_3^0 and χ_4^0 , are singlino- and bino-like, respectively, whose productions are coupling-suppressed. In contrast to scenarios in which the higgsinos do not form the lightest triplet, here one loses out on the cascade of one of the neutralinos (which is the LSP in the present case). This restricts their abilities to contribute to diverse final states. On top of that, χ_1^\pm and χ_2^0 , once produced in such a scenario, decays to

Input/Observables	BP-A1	BP-A2	BP-A3	BP-A4
λ	0.609	0.609	0.633	0.523
κ	0.326	0.326	0.216	0.041
$\tan \beta$	1.98	1.98	1.79	3.65
A_λ (GeV)	477.0	477.0	-558.7	-1253.9
A_κ (GeV)	38.7	37.8	-46.3	138.1
μ_{eff} (GeV)	421.8	421.8	-398.7	-334.5
M_1 (GeV)	480.1	-365.1	286.3	-143.8
$M_{\tilde{Q}_3}$ (GeV)	4262.7	4262.7	3950.3	2292.0
$M_{\tilde{U}_3}$ (GeV)	3450.4	3450.4	3544.4	3435.8
A_t (GeV)	-639.2	-639.2	1372	3862.4
$m_{\chi_1^0}$ (GeV)	395.9	-360.9	284.5	-61.3
$m_{\chi_2^0}$ (GeV)	-445.6	415.1	-289.5	-139.2
$m_{\chi_3^0}$ (GeV)	476.8	-447.5	-421.8	-359.3
$m_{\chi_4^0}$ (GeV)	509.5	493.2	-426.9	359.7
$m_{\chi_5^0}$ (GeV)	2538.7	2538.7	2542.1	2534.2
$m_{\chi_{1,2}^\pm}$ (GeV)	431.5	431.5	-412.1	-345.3
m_{h_1} (GeV)	122.6	122.7	126.9	74.0
m_{h_2} (GeV)	449.2	449.0	288.5	124.7
m_{h_3} (GeV)	822.8	824.8	806.4	1296.6
m_{a_1} (GeV)	75.01	79.0	84.8	121.0
m_{a_2} (GeV)	819.4	821.4	805.4	1296.6
m_{H^\pm} (GeV)	816.5	818.4	800.9	1293.3
$N_{11}, N_{21}, N_{31}, N_{41}$	-0.43, -0.01, -0.62, 0.66	0.995, 0.05, -0.15, 0.02	-0.99, -0.02, -0.06, 0.08	0.12, 0.98, -0.17, 0.04
$N_{13}, N_{23}, N_{33}, N_{43}$	-0.56, -0.70, -0.79, -0.43	0.15, -0.58, 0.69, -0.41	-0.10, -0.06, -0.71, 0.70	0.01, -0.15, -0.70, 0.70
$N_{14}, N_{24}, N_{34}, N_{44}$	0.61, 0.70, -0.06, 0.36	0.07, 0.66, 0.70, 0.27	-0.01, 0.27, 0.67, 0.70	0.25, 0.06, 0.68, 0.69
$N_{15}, N_{25}, N_{35}, N_{45}$	-0.35, 0.11, 0.80, 0.50	0.02, -0.48, 0.11, 0.87	0.02, 0.96, -0.23, -0.15	0.96, -0.14, -0.15, -0.19
$\text{BR}(\chi_1^\pm \rightarrow \chi_1^0 W^\pm)$	off-shell	off-shell	0.14	0.81
$\text{BR}(\chi_1^\pm \rightarrow \chi_2^0 W^\pm)$	off-shell	off-shell	0.86	0.19
$\text{BR}(\chi_2^0 \rightarrow \chi_1^0 h_1)$	off-shell	off-shell	~ 0	0.98
$\text{BR}(\chi_2^0 \rightarrow \chi_1^0 \gamma)$	~ 0.01	0.001	0.98	~ 0
$\text{BR}(\chi_3^0 \rightarrow \chi_1^0 Z)$	off-shell	off-shell	0.06	0.47
$\text{BR}(\chi_3^0 \rightarrow \chi_2^0 Z)$	off-shell	off-shell	0.58	0.05
$\text{BR}(\chi_3^0 \rightarrow \chi_2^0 h_1)$	off-shell	off-shell	0.33	0.03
$\text{BR}(\chi_3^0 \rightarrow \chi_1^0 h_2)$	off-shell	off-shell	~ 0	0.27
$\text{BR}(\chi_3^0 \rightarrow \chi_2^0 h_2)$	off-shell	off-shell	~ 0	0.12
$\text{BR}(\chi_3^0 \rightarrow \chi_1^0 a_1)$	0.23	0.13	0.01	0.01
$\text{BR}(\chi_4^0 \rightarrow \chi_1^0 Z)$	0.14	0.90	0.07	0.37
$\text{BR}(\chi_4^0 \rightarrow \chi_2^0 Z)$	off-shell	~ 0	0.30	0.17
$\text{BR}(\chi_4^0 \rightarrow \chi_1^0 h_2)$	off-shell	~ 0	0	0.32
$\text{BR}(\chi_4^0 \rightarrow \chi_1^0 a_1)$	0.14	0.01	~ 0	0.08
$\text{BR}(\chi_4^0 \rightarrow \chi_2^0 a_1)$	off-shell	~ 0	0.58	0.01
$\text{BR}(H^\pm \rightarrow t\bar{b})$	0.93	0.92	0.84	0.27
Ωh^2	3.78×10^{-4}	0.107	0.119	1.96×10^{-3}
$\sigma_{\chi_1^0-p(n)}^{\text{SI}} \times \xi$ (cm ²)	$1.2(1.3) \times 10^{-46}$	$7.2(7.6) \times 10^{-48}$	$1.2(1.2) \times 10^{-46}$	$4.1(4.3) \times 10^{-47}$
$\sigma_{\chi_1^0-p(n)}^{\text{SD}} \times \xi$ (cm ²)	$4.6(4.5) \times 10^{-44}$	$9.4(7.3) \times 10^{-42}$	$3.5(2.8) \times 10^{-42}$	$1.1(0.8) \times 10^{-41}$
CheckMATE result	Allowed	Allowed	Allowed	Allowed
r -value	0.03	0.08	0.14	0.55
Analysis ID	CMS_SUS_16.039 [167]	CMS_SUS_16.039 [167]	CMS_SUS_16.039 [167]	CMS_SUS_16.039 [167]
Signal region ID	SR_A01	SR_A08	SR_A28	SR_A31

Table 4. Same as in table 3 except for showing benchmark scenarios (with successful nucleation) allowed by all relevant theoretical and experimental constraints including the recent ones from the LHC electroweakino searches. The details of the EWPT are indicated separately in tables 5 and 6.

BM No.	T_i (GeV) (Transition pattern)		$\{h_d, h_u, h_s\}_{\text{false}}$ (GeV)	Transition type	$\{h_d, h_u, h_s\}_{\text{true}}$ (GeV)	γ_{EW} $= \frac{\Delta_{SU(2)}}{T_n}$
BP-A1	T_c	946.7	{0, 0, 0}	FO	{0, 0, 63.2}	1.08
	II-S(1)-D(1)	91.1	{0, 0, 1000.9}	,,	{40.4, 79.6, 1000.7}	
	T_n	946.6	{0, 0, 0}	,,	{0, 0, 64.9}	
	II-S(1)-D(1)	90.2	{0, 0, 1000.9}	,,	{44.2, 86.9, 1000.6}	
BP-A2	T_c	946.0	{0, 0, 0}	,,	{0, 0, 64.4}	1.46
	II-S(1)-D(1)	91.3	{0, 0, 1000.9}	,,	{39.9, 78.6, 1000.6}	
	T_n	945.6	{0, 0, 0}	,,	{0, 0, 66.2}	
	II-S(1)-D(1)	86.2	{0, 0, 1000.8}	,,	{57.1, 112.5, 1000.3}	
BP-A3	T_c	644.4	{0, 0, 0}	,,	{0, 0, -100.0}	1.04
	II-S(1)-D(1)	95.8	{0, 0, -916.3}	,,	{41.4, 72.9, -915.3}	
	T_n	644.3	{0, 0, 0}	,,	{0, 0, -104.8}	
	II-S(1)-D(1)	94.5	{0, 0, -914.9}	,,	{48.5, 85.6, -914.8}	
BP-A4	T_c	185.0	{0, 0, 0}	,,	{0, 0, -668.9}	1.01
	II-S(1)-D(2)	136.5	{0, 0, -846.6}	SO	{2.3, 9.1, -846.7}	
	T_n I-(1)	116.9	{0, 0, 0}	FO	{30.3, 113.8, -877.4}	

Table 5. Phase transition characteristics of the benchmark points presented in table 4. For each benchmark point, presented are the T_c 's and T_n 's, the corresponding field values, the transition types ('FO' for first-order and 'SO' for second-order) and the strengths of the phase transition along the $SU(2)$ -direction (γ_{EW}). See text for details.

the LSP, which is not far away in mass, via off-shell gauge and Higgs bosons (as indicated in table 4) thus resulting in associated leptons/jets to be generically soft. Both these issues have negative impacts on the experimental sensitivities of such a scenario. This is clearly reflected in the LHC analyses of such scenarios [125, 126] which report much relaxed lower bounds (down to ~ 220 GeV, conservatively) on the masses of such higgsino-like electroweakinos as a function of their mass-split with the LSP.

A CheckMATE analysis that includes all readily available analyses in its repository results in a ' r ' value far below 1 for the point BP-A1 thus marking its total insensitivity to the LHC searches and hence allowed by the same. The relevant analysis and the most significant signal region therein are also indicated. Note that the higgsino masses for this benchmark point are way above their current lower bounds for such a scenario as mentioned above. In passing, we note that in the future runs of the LHC such a scenario would likely attract bounds from the searches of the doublet-like heavy Higgs bosons sooner than from the direct searches for such electroweakinos.

Benchmark point BP-A2 is almost the same as BP-A1 except for M_1 now being brought

down below μ_{eff} . Thus, the LSP DM is now highly bino-dominated and its relic abundance ($\Omega h^2 = 0.107$) now falls within the Planck-observed band. Towards this, the required depletion in the relic is again facilitated by the coannihilation of the bino-like DM with the higgsino-like chargino and neutralinos. Note that the sign on M_1 (with respect to that of μ_{eff}) ensures compliance with the experimentally observed latest upper bound on the DMDD-SI cross-section by setting up a so-called ‘coupling blind spot’ as discussed in section 3.2.2.

As in BP-A1, EWPT in BP-A2 is also of the type II-S(1)-D(1). The only notable difference that is found with respect to BP-A1 is in the delayed nucleation for the crucial phase transition in the $SU(2)$ field directions ($T_n = 86.2$ GeV, as opposed to 90.2 GeV in BP-A1) as shown in table 5. This results in a stronger FOEWPT ($\gamma_{EW} = 1.5$, compared to $\gamma_{EW} = 1.1$ in BP-A1). Its implications for the GW physics will be discussed in section 4.3.3. The delayed nucleation can be explained by the altered M_1 which modifies the thermal correction to the effective potential via terms that are only quadratic and quartic in $m(\phi)/T$ given that the bino is a fermion (see equation 3.5b). For our present benchmark scenario, successful nucleation would then require some appropriate modification in the term cubic in $m(\phi)/T$ which we achieve by a minor tweaking of A_κ . In the process, the potential barrier gets modified in a way that leads to delayed nucleation compared to BP-A1.

On the LHC front, unlike in BP-A1, in BP-A2 cascades of both higgsino-like neutralinos ($\chi_{2,3}^0$) will be important for the relevant final states. Although, just as in BP-A1, $\chi_{2,3}^0$ and the higgsino-like χ_1^\pm would undergo off-shell decays to Z , h_{SM} and W^\pm , the corresponding branching fractions for $\chi_{2,3}^0$ get suppressed in the presence of their significant on-shell branchings to a photon (for χ_2^0) and to a light a_s (for χ_3^0). The relevant lower bound from the LHC on the masses of lighter electroweakinos with such mass-splits is presented in reference [125] for a wino(NLSP)-bino(LSP) system which can be conservatively taken as ~ 300 GeV. In a scenario like BP-A2, such a bound would get weakened not only because of the suppressed off-shell branching fractions of the neutralinos as mentioned above but also, as described in section 3.2.2, since the collective production cross-sections for the higgsino-like electroweakinos are known to be smaller than if they were wino-like, for any given mass. This is corroborated by our CheckMATE analysis which indeed allows BP-A2. Compressed scenarios like BP-A1 and BP-A2 would, however, be sensitive to the HL-LHC. Also, as for BP-A1, BP-A2 is likely to be probed first in the searches for doublet-like heavy Higgs bosons at future LHC runs.

The benchmark point BP-A3, to start with, differs from BP-A2 in having a light singlino-like (NLSP, χ_2^0) state in-between the bino-like LSP (χ_1^0) and the higgsino-like chargino (χ_1^\pm) and neutralinos $\chi_{3,4}^0$. This is achieved by lowering the ratio κ/λ . The split between χ_2^0 and χ_1^0 is tailored to be rather small (~ 5 GeV). Expectedly, the abundance of the highly bino-dominated LSP DM depletes via its coannihilation with the singlino-dominated NLSP. The DM relic abundance is found to lie within the Planck-observed band. Note that the proximity in the masses of these two states could, apriori, infuse a significant singlino component within the LSP thus pushing up the DMDD-SI cross sections dangerously. For the current benchmark scenario, such contamination has been tamed by requiring a relative sign between M_1 and $m_{\tilde{s}} (= 2\kappa\mu_{\text{eff}}/\lambda)$ [122]. Achieving the coveted relative sign between these two quantities

through a relative sign between M_1 and μ_{eff} has an additional advantage since, as in BP-A2, this further helps restrict the DMDD-SI cross-section below its experimentally observed upper limit. The pattern of EWPT in BP-A3 is pretty similar to those in BP-A1 and BP-A2, i.e., this is a two-step process of type II-S(1)-D(1). However, the first transition along the singlet direction occurs somewhat later in time at around 644 GeV (in place of 945 GeV, as in BP-A2).

On the collider front, the higgsino-like $\chi_{3,4}^0$ (χ_1^\pm) preferentially decay to singlino-like NLSP, χ_2^0 (thanks to their enhanced coupling given ‘ λ ’ is reasonably large [122]) along with an on-shell Z -boson and Higgs bosons (W^\pm boson). In turn, it is found that χ_2^0 dominantly decays to $\chi_1^0\gamma$ ($\sim 98\%$) as its decays to off-shell Z - and Higgs bosons are much suppressed due to a small mass-split between χ_2^0 and the LSP. Conservatively, when such photons go undetected due to their softness, cascades of the higgsino-like states via χ_2^0 would be effectively equivalent to their direct decays to LSP thus resulting in canonically sensitive final states like $3\ell + \cancel{E}_T$ and $1\ell + 2b\text{-jets} + \cancel{E}_T$. Hence the reported bounds on the masses of the wino-like electroweakinos from such final states, after correcting (relaxing) for the higgsino-like ones, would hold straightaway. Our CheckMATE analysis shows that BP-A3 survives with this bound and is expected to be probed at the HL-LHC via the above standard searches for the electroweakinos as well as in the hunt for doublet-like heavier Higgs bosons.

The benchmark point BP-A4 differs from BP-A3 in the flipping of the nature of the LSP and NLSP, i.e., the LSP (NLSP) becomes singlino-dominated (bino-dominated). Furthermore, this is the only benchmark point where we find the CP -even singlet Higgs boson to be the lightest of the scalars ($h_s \sim 74$ GeV). Also, BP-A4 contains the smallest $|\mu_{\text{eff}}|$ (~ 335 GeV) among all four benchmark points presented in this table. The DM is found to be underabundant in the presence of multiple funnels (a_s and h_{SM}). Hence the DMDD bounds are again satisfied thanks to the downward scaling of the DD cross sections.

The EWPT still takes place in two steps but is of type II-S(1)-D(2) as is suggested by the calculations of T_c . The first of these is of the strong first-order type occurring along the singlet-direction at $T_c = 165$ GeV. The subsequent transition occurs along the $SU(2)$ direction at $T_c = 136.5$ GeV and second-order in nature. However, the nucleation calculation indicates that the tunneling rate corresponding to the first transition is too small. Consequently, the actual nucleation from the trivial phase to the physical phase takes place directly (type I-(1)) at a later time at $T_n = 116.9$ GeV. The possibility of such kind of a phase transition has already been pointed out in reference [54].

As in BP-A3, heavier higgsinos, $\chi_{3,4}^0$, decay to a bino-dominated NLSP (χ_2^0) and a singlino-dominated LSP (χ_1^0) accompanied by an on-shell gauge or a Higgs boson. Here also, $\chi_{3,4}^0$ ’s decays to the singlino-dominated state (the LSP in this case) are favored as ‘ λ ’ is on the larger side. On the other hand, the bino-dominated χ_2^0 now undergoes a dominant decay to the singlet-like CP -even Higgs boson h_s and the singlino-dominated χ_1^0 . This can play a crucial role in relaxing the relevant collider bounds [122, 197] when the heavier higgsinos first decay to χ_2^0 which all have branching fractions around 20% for the present benchmark point (see table 4).

Among the implemented analyses in the CheckMATE package an older CMS one (with

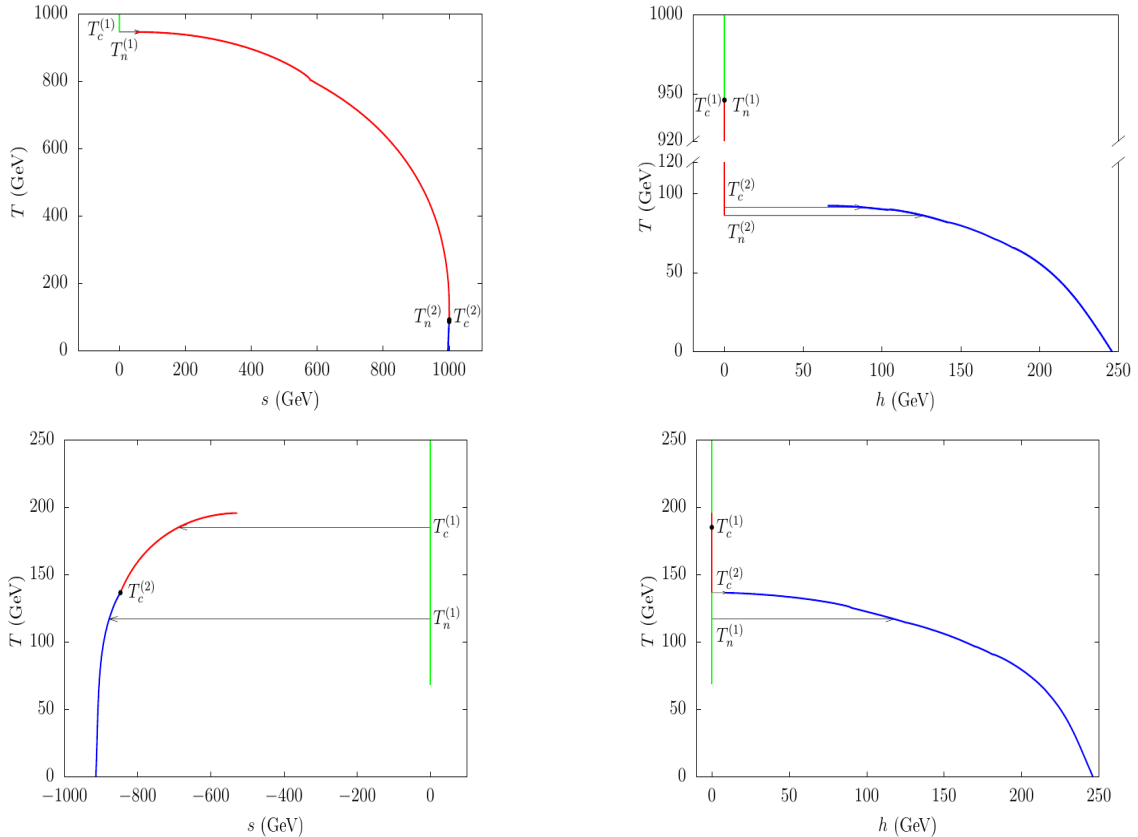


Figure 2. Phase flows in benchmark scenarios BP-A2 and BP-A4. Each color stands for a particular minimum of the potential (phase) while the individual lines represent the evolution of the phase in different field directions (along the singlet direction s (left) and along the $SU(2)$ -direction $h = \sqrt{h_d^2 + h_u^2}$ (right)) as a function of temperature. For each phase transition denoted are the T_c and T_n . The arrows represent the directions of transition from the false to the true vacuum as obtained from the calculations at T_c and T_n in the corresponding field space whereas a bullet in black denotes that along this transition the corresponding field value does not alter too much. $T_{c,n}^{(i)}$ ($i \in \{1, 2\}$) stands for i -th transition from the calculation of $T_{c,n}$.

35.9 fb $^{-1}$ of data) [167] and another from the ATLAS (with 139 fb $^{-1}$ of data) [180] show maximal sensitivities in the final states with $3\ell + \cancel{E}_T$ and $1\ell + 2\gamma + \cancel{E}_T$, respectively. The corresponding ‘ r ’ values are found to be 0.55 and 0.53 which signify that the BP-A4 is still allowed by a wide margin by the electroweakino searches at the LHC. This may not be unexpected given that the heavier higgsinos do not always undergo one-step decays to the LSP as is assumed by the experimental collaborations. A subsequent analysis with `SModelS` that incorporates very recent ATLAS studies for the final states like $1\ell + h_{\text{SM}}(\rightarrow bb) + \cancel{E}_T$ [176], $2\ell + \cancel{E}_T$ [178] and $3\ell + \cancel{E}_T$ [177] with 139 fb $^{-1}$ of data keeps this benchmark point alive.

In this regard, recent analyses by the ATLAS and the CMS collaborations of the final state $3\ell + \cancel{E}_T$, with and without extra jets, at 139 fb $^{-1}$ and 137 fb $^{-1}$ of data, respectively [125, 186], are expected to have heightened sensitivities to the present benchmark scenario but are

BP No.	T_n (GeV)	α	β/H_n
BP-A1	946.7	2.04×10^{-5}	1.31×10^7
	90.2	2.34×10^{-2}	2.53×10^4
BP-A2	945.9	2.15×10^{-5}	1.19×10^7
	86.2	4.33×10^{-2}	1.21×10^3
BP-A3	644.3	1.12×10^{-4}	2.06×10^6
	95.2	1.82×10^{-2}	3.71×10^4
BP-A4	116.9	8.63×10^{-2}	2.22×10^2

Table 6. Values of the parameters T_n , α and β/H_n (that control the GW intensity) for the benchmark points presented in table 4.

yet to be implemented in the recast packages. However, we have managed to check the constraints from the ATLAS analysis [125] for this benchmark scenario and we find [199] BP-A4 to be still allowed. The scenario is expected to get probed at the future LHC runs in the electroweakino searches first rather than in the searches for the heavy Higgs bosons. This is since these doublet-like heavy Higgs bosons are heavier in the present case (~ 1.3 TeV).

As we have just discussed, benchmark points BP-A1, BP-A2, and BP-A3 have similar phase transition patterns while BP-A4 has one of a different kind. Hence, in figure 2, we choose to show the relevant phase diagrams for only BP-A2 (having an SFOEWPT in two steps with a palpable split between T_c and T_n) and BP-A4 (one-step phase transition with a reasonably large T_c and T_n for the SFO) which may serve as the representative scenarios for the purpose.

4.3.3 Prospects of GW detection

Values of various key parameters (T_n , α , β/H_n) pertaining to the GW spectra arising from the FOPTs for the benchmark scenarios BP-A1 to BP-A4 are shown in table 6. The corresponding GW (frequency) spectra are calculated using equations 3.8–3.16 and are shown in figure 3. These are further compared with the sensitivity of some space- and ground-based gravitational wave detectors, viz., LISA [200], Taiji [201], TianQin [202], aLigo+ [203], Big Bang Observer (BBO) [204] and Ultimate(U)-DECIGO [205]. The contributions from sound waves and turbulence for each phase transition process are shown in different colors with broken lines. Note that for each of the benchmark points BP-A1, BP-A2 and BP-A3 we observe a two-step phase transition as can be gleaned from figure 3. In all these three cases, the right (left) humps correspond to the peak frequency of the first (second) FOPT. Contribution from MHD turbulence from the first FOPT (along the singlet direction), for each of these three benchmark scenarios, does not appear explicitly in these plots since its relative strength is much too small. Note that for each of these scenarios, phase transitions along the singlet-

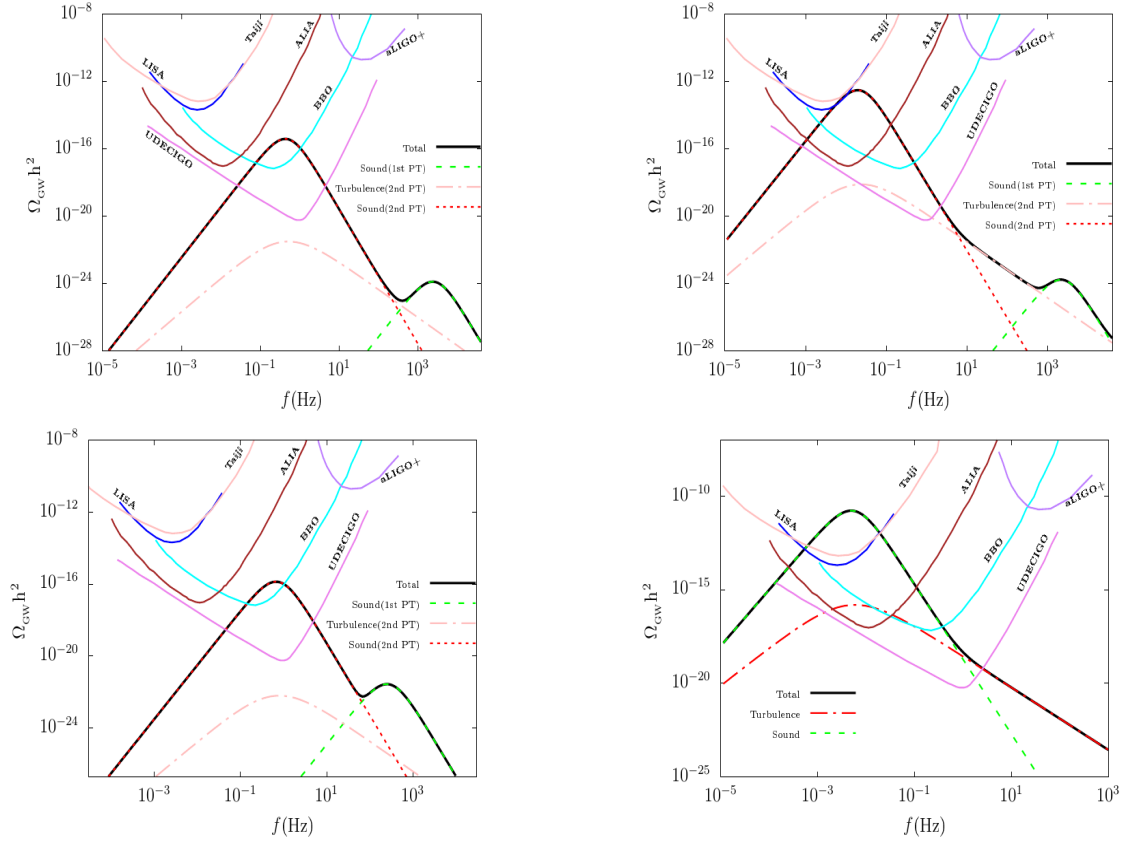


Figure 3. GW energy density spectrum with respect to frequency for the four benchmark scenarios BP-A1 (top, left), BP-A2 (top, right), BP-A3 (bottom, left) and BP-A4 (bottom, right) illustrated against the experimental sensitivity curves of some GW detectors like LISA, Taiji, TianQin, aLigo+, BBO and U-DECIGO. In each plot, the black line denotes the total GW energy density obtained for the particular benchmark scenario whereas the broken lines in various colors represent individual contributions from sound waves and turbulence for different phase transitions. Note that the turbulence contributions from the first FOPT (along the singlet direction) for the benchmark scenarios BP-A1, BP-A2 and BP-A3 do not appear in these plots as their contributions are too small.

direction happen at relatively larger temperatures (happens to be at larger β/H_n values). Hence the shorter peaks (from the first transitions, for the cases in hand) do not fall inside the projected design-sensitivity of the future GW experiments.⁶ We reserve this study for a future work. On the other hand, in BP-A4 SFOPT occurs in a single step which can be seen in the bottom, right plot of figure 3. Note that the GW intensity obtained for BP-A1 lies within the sensitivities of BBO and U-DECIGO while for BP-A2 the same lies within the sensitivity of ALIA as well and also marginally gets within that of LISA. Given that

⁶An interesting situation with a GW spectrum having multiple peaks (from a two-step phase transition in the NMSSM) could be observed in these experiments if the transition along the singlet direction also takes place at $T_n \sim 100$ GeV (which enhances the corresponding ‘ α ’ value) and with a relatively smaller value of β/H_n .

these two scenarios have otherwise very similar types of phase transitions, the reason behind the latter can be traced back to the fact that in BP-A2 there occurs a stronger FOPT in the $SU(2)$ field directions due to a relatively late-time nucleation and the associated values taken by ‘ α ’ and β/H_n are such that the GW peak intensity shoots up thus increasing the prospects of observing the same. In contrast, for BP-A4, a section of the GW spectrum falls within the reaches of multiple experiments like LISA, Taiji, ALIA, BBO and U-DECIGO.

The quantity signal-to-noise ratio (SNR) is used to measure the detectability of the GW signal at the experiments. SNR is defined as [127]

$$\text{SNR} = \sqrt{\delta \times \mathcal{T} \int_{f_{min}}^{f_{max}} df \left[\frac{h^2 \Omega_{\text{GW}}(f)}{h^2 \Omega_{\text{exp}}(f)} \right]^2}, \quad (4.1)$$

where \mathcal{T} is the duration of the experimental mission in years, δ stands for the number of independent channels employed by an experiment to exploit cross-correlations (required to pin down the stochastic origin of the GW) and $\Omega_{\text{exp}}(f) h^2$ denotes the effective power spectral density of strain noise of the experiment. Here, we consider $\delta = 2$ for BBO and U-DECIGO and $\delta = 1$ for LISA while for all of them we take $\mathcal{T} = 5$. The SNR values for the benchmark points are found to be way below 1, with the exception of BP-A4, for which it is comparatively large but still $\lesssim 1$. These are to be compared with the reference minimum threshold value of SNR for the detection of GW which is taken to be 10 [127]. Thus, none of the benchmark scenarios meets this detectability criterion. It is, however, expected that there is a region of parameter space in the NMSSM which might give rise to stronger FOPTs (larger α) and the corresponding GW spectra lie deeper within the regions of experimental sensitivity (depending upon β/H_n) thus yielding an SNR value larger than 10.⁷

5 Summary and outlook

Inspired by the prospects the Z_3 -NMSSM scenario holds in explaining the baryon asymmetry of the Universe via EWBG, which in turn requires SFOEWPT, we have sought to figure out how accommodating the scenario appears in the face of recent LHC results, in particular, the ones pertaining to the searches of the lighter electroweakinos which might happen to be higgsino-like and are favored by SFOEWPT. Various pertinent theoretical requirements, constraints on the Higgs sector (including the observed properties of the SM-like Higgs boson) from the LHC, flavor-constraints and bounds on various DM observables obtained from a host of dedicated experiments do already play their parts in delineating the allowed region of the NMSSM parameter space that still remains compatible with SFOEWPT. We further look into the prospects of detecting the (stochastic) GW arising from an SFOEWPT at various future experiments.

The backdrop of our present study has been the looming tension between the physics of SFOEWPT and the recent LHC results from the electroweakino searches. While the former prefers μ_{eff} in the range of a few hundreds of a GeV, the latter are tending to push μ_{eff} steadily above such a ballpark. The general goal of such a study could then be to check if

⁷The exploration, however, demands a more detailed study which we will take up in a future work.

there is a meeting ground somewhere in the middle where both constraints are simultaneously complied with. A further observation is that EWPT is somewhat stubborn in its need for relatively small μ_{eff} . A middle ground can thus only be found if the reported constraints from the LHC could be evaded under circumstances that have not been considered explicitly by the LHC experiments. In this work, we exploit such caveats to our advantage via recasts of the relevant LHC analyses using popular packages like **CheckMATE** and **SModelS**.

Thus, the region of the Z_3 -NMSSM parameter space that concerns us in this work is characterized by reasonably small μ_{eff} that yields relatively light higgsino-like states. Also, SFOEWPT prefers a relatively light CP -even singlet-like scalar, h_s , thus requiring ‘ κ ’ to be small. This leads to a relatively light singlino in the spectrum which can be the DM particle while the light singlet scalars play crucial roles in the DM phenomenology. Also, for our benchmark scenarios, we choose relatively large values of ‘ λ ’ ($\gtrsim 0.5$) and smaller values of $\tan\beta$ ($\lesssim 5$). Together, these yields $m_{h_{\text{SM}}}$ in the right ballpark (~ 125 GeV) without requiring too large SUSY radiative corrections. Furthermore, a smaller $\tan\beta$ could allow the heavier doublet Higgs bosons to remain relatively light (reminiscent of the “alignment without decoupling” scenario) which might aid SFOEWPT. With ‘ λ ’ on the larger side, the mixing among the higgsinos and the singlino, all of which can be relatively light thus being the candidates for the LSP DM and the NLSP, can be sizable. Hence, with such choices of theory parameters, the physics of the EWPT (and hence EWBG) becomes intricately connected to the DM and collider (LHC) phenomenologies.

Results of a scan over the parameter space are presented depicting first how relatively small μ_{eff} ($\lesssim 500$ GeV) fares against various theoretical and basic experimental bounds including those from the observed Higgs sector and the ones from the DM experiments. Two sets of benchmark scenarios are then presented to demonstrate the SFOEWPT–DM–LHC connection. These scenarios are checked to give rise to SFOEWPT by using the package **CosmoTransitions** in which we implemented the framework of Z_3 -NMSSM, matched to THDMs, as has been a pretty standard practice for the purpose.

With one set of benchmark scenarios, we have sought to find out up to what a ballpark maximum value of not so large a μ_{eff} can still be ruled out by recent LHC analyses, in particular, when one departs from the simplified assumptions on the decays and branching fractions of the cascading electroweakinos which is expected to relax the reported bounds on the electroweakino masses. Subjecting this set of otherwise highly motivated scenarios to thorough recasts of some pertinent LHC analyses (with both 36 fb^{-1} and 139 fb^{-1} of data) with the help of **CheckMATE** and **SModelS** reveals that $\mu_{\text{eff}} \lesssim 300$ GeV, with low values of ‘ κ ’ ($\lesssim 0.1$) and larger ‘ λ ’ ($\gtrsim 0.5$), is mostly ruled out. It should be noted that smaller values of μ_{eff} already attract severe constraints from the DM direct detection experiments. Thus, in this regard, the LHC searches might not always yield a robust improvement over the DM bounds. An even smaller μ_{eff} could, however, survive the LHC bounds for a compressed electroweakino spectrum. In this work, being conservative, we do not consider this possibility.

With the other set of benchmark scenarios, we have demonstrated how low a μ_{eff} could still be allowed instead. A similar exercise shows that, under favorable circumstances, upwards of $\mu_{\text{eff}} \sim 335$ GeV could survive the LHC onslaught. This is rather encouraging since

we find that EWPT could still remain to be of strong, first-order type even for μ_{eff} as large as ~ 425 GeV which is the case for a couple of benchmark scenarios that we have presented. These also show that a viable LSP DM can be bino- or singlino-like or even a mixture of bino, singlino and higgsino states. We have thoroughly studied the properties of EWPT in these scenarios with the help of `CosmoTransitions` and have found that for μ_{eff} on the larger side, a two-step phase transition is a more likely phenomenon with the first transition taking place in the singlet field direction followed by the other in the $SU(2)$ field directions.

For these latter set of scenarios, we have thoroughly studied the stochastic GW (background) spectra that might carry the imprints of FOPT from new physics beyond the SM. We find that the signal intensities lie inside the sensitivity limits of one or more of the future/proposed experiments like the LISA, BBO, UDECIGO, Taiji, Alia, etc. However, the SNR values, as such, are not found to be healthy enough to guarantee a positive detection.

In summary, the present work corroborates the basic findings reported in the literature pertaining to SFOEWPT, in particular, and EWPT, in general, in the framework of the Z_3 -NMSSM. We broadly concur with various reported patterns and features of EWPT in such a scenario and the different conditions under which those manifest. We then go beyond to shed light on what the recent searches of the electroweakinos at the LHC have to say about the viability of SFOEWPT in the current framework while compatibility with the constraints from various pertinent theoretical and experimental sectors including the DM sector is ensured all through. Furthermore, it appears that the GW signals resulting from the strong FOPTs in these scenarios are likely to remain too weak to be detected at future dedicated experiments.

As for an outlook, new LHC studies with data from the recently terminated LHC Run 2 and those that would arrive soon from high luminosity LHC (HL-LHC) are likely to shed a more unambiguous light on the broad viability of EWBG within the Z_3 -NMSSM while these continue to explore electroweakinos at larger masses and in difficult scenarios like the compressed ones. Furthermore, improvements are possible in the theoretical calculations of several key EWBG objects, viz., the bubble wall profile, wall velocity and CP -violation and in the dealing of the transport equations which could lend a more accurate estimate of the relation between the NMSSM parameters and EWBG. With these, a reassessment of the detectability of such GW signals may be warranted which might prove the latter's role as complementary to the LHC searches. A synergy like this between LHC and GW physics is likely to be rather intriguing and we reserve such a study for a future work.

6 Acknowledgments

AC thanks Harish-Chandra Research Institute (HRI) for hosting him during the course of this collaborative work. AC also acknowledges partial support from the Department of Science and Technology, India, through INSPIRE faculty fellowship (grant no: IFA 15 PH-130, DST/INSPIRE/04/2015/000110). SR is supported by the funding available from the Department of Atomic Energy (DAE), Government of India for the Regional Centre for Accelerator-based Particle Physics (RECAPP) at HRI. SR would like to thank Peter Athron, Sebastian

Baum, Junji Cao, Ulrich Ellwanger, Andrew Fowlie, Tathagata Ghosh, Sabine Kraml, Indrani Pal, Avik Paul, Krzysztof Rolbiecki, Tim Stefaniak, Di Zhang, Yang Zhang for helpful discussions and communications. SR also acknowledges the use of cluster computing available at the High Performance Scientific Computing facility at HRI and thanks Rajiv Kumar for his technical help at this facility.

Appendices

A Matching the NMSSM parameters to those in the THDMS potential

In terms of the CP -even Higgs fields h_d , h_u and s , the tree-level Z_3 -NMSSM potential of equation 2.3, which is relevant for the study of phase transitions, can be written as [48]

$$V_{\text{tree}}^{\text{NMSSM}}(h_d, h_u, s) = \frac{1}{32}(g_1^2 + g_2^2)(h_d^2 - h_u^2)^2 + \frac{1}{4}\kappa^2 s^4 - \frac{1}{2}\lambda\kappa s^2 h_d h_u + \frac{1}{4}\lambda^2 [h_d^2 h_u^2 + s^2(h_d^2 + h_u^2)] - \frac{1}{\sqrt{2}}\lambda A_\lambda s h_d h_u + \frac{1}{3\sqrt{2}}\kappa A_\kappa s^3 + \frac{1}{2}m_{H_d}^2 h_d^2 + \frac{1}{2}m_{H_u}^2 h_u^2 + \frac{1}{2}m_S^2 s^2. \quad (\text{A.1})$$

On the other hand, the tree-level Z_3 -symmetric THDMS potential is given by [52, 105–107]

$$V_{\text{tree}}^{\text{THDMS}} = \frac{1}{2}\lambda_1 |H_d|^4 + \frac{1}{2}\lambda_2 |H_u|^4 + (\lambda_3 + \lambda_4) |H_d|^2 |H_u|^2 - \lambda_4 |H_u^\dagger H_d|^2 + \lambda_5 |H_d|^2 |S|^2 + \lambda_6 |H_u|^2 |S|^2 + \lambda_7 (S^{*2} H_d \cdot H_u + \text{h.c.}) + \lambda_8 |S|^4 + m_1^2 |H_d|^2 + m_2^2 |H_u|^2 + m_3^2 |S|^2 - m_4 (H_d \cdot H_u S + \text{h.c.}) - \frac{1}{3}m_5 (S^3 + \text{h.c.}). \quad (\text{A.2})$$

All parameters in equation A.1 and A.2 are taken to be real as we do not consider any CP -violation in the Higgs sector in this work. We use `NMSSMTools` to obtain the particle spectrum of the Z_3 -NMSSM at the scale M_{SUSY} . Except for the electroweakinos with masses around a few hundred GeV, we consider all other SUSY excitations to be much heavier such that those may be considered effectively decoupled from the physics of phase transitions. However, to avoid large logarithmic corrections from appearing in $V_{\text{CW}}^{\text{NMSSM}}$ due to the top squarks, those are integrated out at the scale M_{SUSY} in an EFT approach. Below this scale, $V_{\text{tree}}^{\text{NMSSM}}$ can be mapped onto $V_{\text{tree}}^{\text{THDMS}}$. Comparing equations A.1 and A.2, after expanding the latter in terms of the component fields h_d, h_u and ‘ s ’, the matched conditions among the model parameters of these two scenarios, at the scale M_{SUSY} , are given by [52, 105–107]

$$\begin{aligned} \lambda_1 = \lambda_2 &= \frac{1}{4}(g_1^2 + g_2^2), & \lambda_3 &= \frac{1}{4}(g_2^2 - g_1^2), \\ \lambda_4 &= \frac{1}{2}(2|\lambda|^2 - g_2^2), & \lambda_5 = \lambda_6 &= |\lambda|^2, & \lambda_7 &= -\lambda\kappa, & \lambda_8 &= |\kappa|^2, \\ m_1^2 = m_{H_d}^2, & m_2^2 = m_{H_u}^2, & m_3^2 &= m_S^2, & m_4 &= A_\lambda \lambda, & m_5 &= -A_\kappa \kappa. \end{aligned} \quad (\text{A.3})$$

At one-loop, the only relevant threshold correction that arises (as the top squarks are integrated out at the scale M_{SUSY}) is to λ_2 and is given by [206–209]

$$\Delta\lambda_2 = \frac{3y_t^4 A_t^2}{8\pi^2 M_{\text{SUSY}}^2} \left(1 - \frac{A_t^2}{12M_{\text{SUSY}}^2} \right), \quad (\text{A.4})$$

where A_t is the soft-SUSY-breaking top squark-Higgs trilinear coupling in the scalar potential and y_t is the top quark Yukawa coupling, both defined at the scale M_{SUSY} . Note that all the NMSSM parameters are also provided at the scale M_{SUSY} and in the $\overline{\text{DR}}$ scheme. Thus, after matching, all the THDMS parameters also get defined at the same scale and in the same renormalization scheme.

B RGEs in the THDMS

We borrow the set of relevant RGEs from reference [37] which we use to run the THDMS model parameters from the scale M_{SUSY} to the scale m_t . Contributions to the β -functions from the SM gauge bosons, the Higgs bosons, the top quark, the higgsinos and the singlino are included. As for the gauginos, the contribution from the bino is known to be small (even when M_1 does not get to be too large, as is the case in our present analysis) while M_2 is set at a rather large value. Hence we ignore their effects. With these, the one-loop β -functions for the model parameters q_i are given by

$$\beta_{q_i} = \frac{1}{16\pi^2} \frac{\partial}{\partial \ln \Lambda} q_i, \quad (\text{B.1})$$

where ‘ Λ ’ is the energy scale. The one-loop RGEs for the quartic couplings $\lambda_i, i \in \{1, 2, 3, \dots, 8\}$, the mass parameters $(m_{4,5})$ and v_s appearing in $V_{\text{tree}}^{\text{THDMS}}$ of equation A.2 are as follows [37, 48, 105]:

$$\begin{aligned} \beta_{\lambda_1} &= 12\lambda_1^2 + 4\lambda_3^2 + 4\lambda_3\lambda_4 + 2\lambda_4^2 + 2\lambda_5^2 - \lambda_1(3g_1^2 + 9g_2^2) + \frac{3}{4}g_1^4 + \frac{9}{4}g_2^4 + \frac{3}{2}g_1^2g_2^2 - 4\lambda^4 + 4\lambda^2\lambda_1, \\ \beta_{\lambda_2} &= 12\lambda_2^2 + 4\lambda_3^2 + 4\lambda_3\lambda_4 + 2\lambda_4^2 + 2\lambda_6^2 - \lambda_2(3g_1^2 + 9g_2^2) + \frac{3}{4}g_1^4 + \frac{9}{4}g_2^4 + \frac{3}{2}g_1^2g_2^2 + 12y_t^2\lambda_2 - 12y_t^4 \\ &\quad - 4\lambda^4 + 4\lambda^2\lambda_2, \\ \beta_{\lambda_3} &= (\lambda_1 + \lambda_2)(6\lambda_3 + 2\lambda_4) + 4\lambda_3^2 + 2\lambda_4^2 + 2\lambda_5\lambda_6 - \lambda_3(3g_1^2 + 9g_2^2) + \frac{3}{4}g_1^4 + \frac{9}{4}g_2^4 - \frac{3}{2}g_1^2g_2^2 + 6y_t^2\lambda_3 \\ &\quad - 4\lambda^4 + 8\lambda^2\lambda_4 + 8\lambda^2\lambda_3, \\ \beta_{\lambda_4} &= 2\lambda_4(\lambda_1 + \lambda_2 + 4\lambda_3 + 2\lambda_4) + 4\lambda_7^2 - \lambda_4(3g_1^2 + 9g_2^2) + 3g_1^2g_2^2 + 6y_t^2\lambda_4 + 4\lambda^4 - 4\lambda^2\lambda_4, \\ \beta_{\lambda_5} &= \lambda_5(6\lambda_1 + 4\lambda_5 + 8\lambda_8) + \lambda_6(4\lambda_3 + 2\lambda_4) + 8\lambda_7^2 - \frac{1}{2}\lambda_5(3g_1^2 + 9g_2^2) - 12\kappa^2\lambda^2 - 4\lambda^4 + 4\kappa^2\lambda_5 + 6\lambda^2\lambda_6, \\ \beta_{\lambda_6} &= \lambda_5(4\lambda_3 + 2\lambda_4) + \lambda_6(6\lambda_2 + 4\lambda_6 + 8\lambda_8) + 8\lambda_7^2 - \frac{1}{2}\lambda_6(3g_1^2 + 9g_2^2) + 6y_t^2\lambda_6 - 16\kappa^2\lambda^2 - 4\lambda^4 \\ &\quad + 4\kappa^2\lambda_6 + 6\lambda^2\lambda_6, \\ \beta_{\lambda_7} &= \lambda_7(2\lambda_3 + 4\lambda_4 + 4\lambda_5 + 4\lambda_6 + 4\lambda_8) - \frac{1}{2}\lambda_7(3g_1^2 + 9g_2^2) + 3y_t^2\lambda_7 + 8\kappa\lambda^3 + 4\kappa^2\lambda_7 + 6\lambda^2\lambda_7, \\ \beta_{\lambda_8} &= 2\lambda_5^2 + 2\lambda_6^2 + 4\lambda_7^2 + 20\lambda_8^2 + 8(\kappa^2 + \lambda^2)\lambda_8 - 16\kappa^2 - 4\lambda^4, \\ \beta_{m_4} &= (2\lambda_3 + 4\lambda_4 + 2\lambda_5 + 2\lambda_6 + 4\lambda^2 + 2\kappa^2 - \frac{9}{2}g_2^2 - \frac{3}{2}g_1^2 + 3y_t^2)m_4 + 4\lambda_7m_5, \\ \beta_{m_5} &= (12\lambda_8 + 6\lambda^2 + 6\kappa^2)m_5 + 12\lambda_7m_4, \\ \beta_{v_s} &= -2v_s(\kappa^2 + \lambda^2). \end{aligned} \quad (\text{B.2})$$

The individual THDMS parameters at the scale m_t are then calculated using the expression⁸ (see reference [37] for details)

$$q_i(m_t) \simeq q_i(M_{\text{SUSY}}) - \beta_{q_i} \ln \frac{M_{\text{SUSY}}}{m_t}. \quad (\text{B.3})$$

C Field-dependent masses and the daisy corrections

Here we present the field-dependent mass-squared matrices for the scalar sector which are derived from equation A.2 [52, 105]. The 3×3 , symmetric matrix (\mathcal{M}_H^2) for the CP -even scalars, in the basis $\{h_d, h_u, s\}$, is given by

$$\begin{pmatrix} m_1^2 + \frac{3}{2}\lambda_1 h_d^2 + \frac{1}{2}\lambda_5 s^2 + \frac{1}{2}(\lambda_3 + \lambda_4)h_u^2 & -\frac{1}{\sqrt{2}}m_4 s + \frac{1}{2}\lambda_7 s^2 + (\lambda_3 + \lambda_4)h_u h_d & -\frac{1}{\sqrt{2}}m_4 h_u + \lambda_5 h_d s + \lambda_7 h_u s \\ \dots & m_2^2 + \frac{3}{2}\lambda_2 h_u^2 + \frac{1}{2}\lambda_6 s^2 + \frac{1}{2}(\lambda_3 + \lambda_4)h_d^2 & -\frac{1}{\sqrt{2}}m_4 h_d + \lambda_7 h_d s + \lambda_6 h_u s \\ \dots & \dots & m_3^2 - \sqrt{2}m_5 s + \frac{1}{2}\lambda_5 h_d^2 + \lambda_7 h_u h_d + \frac{1}{2}\lambda_6 h_u^2 + 3\lambda_8 s^2 \end{pmatrix}, \quad (\text{C.1})$$

whereas, the corresponding one for the CP -odd scalars (\mathcal{M}_A^2), in the same basis as above, can be written as

$$\begin{pmatrix} m_1^2 + \frac{1}{2}\lambda_1 h_d^2 + \frac{1}{2}\lambda_5 s^2 + \frac{1}{2}(\lambda_3 + \lambda_4)h_u^2 & \frac{1}{\sqrt{2}}m_4 s - \frac{1}{2}\lambda_7 s^2 & \frac{1}{\sqrt{2}}m_4 h_u + \lambda_7 h_u s \\ \dots & m_2^2 + \frac{1}{2}\lambda_2 h_u^2 + \frac{1}{2}\lambda_6 s^2 + \frac{1}{2}(\lambda_3 + \lambda_4)h_d^2 & \frac{1}{\sqrt{2}}m_4 h_d + \lambda_7 h_d s \\ \dots & \dots & m_3^2 + \sqrt{2}m_5 s + \frac{1}{2}\lambda_5 h_d^2 - \lambda_7 h_u h_d + \frac{1}{2}\lambda_6 h_u^2 + \lambda_8 s^2 \end{pmatrix}. \quad (\text{C.2})$$

On the other hand, the field-dependent 2×2 , symmetric mass-squared matrix for the charged Higgs sector ($\mathcal{M}_{H^\pm}^2$) in the basis $\{h_d, h_u\}$ is given by

$$\mathcal{M}_{H^\pm}^2 = \begin{pmatrix} m_1^2 + \frac{1}{2}\lambda_5 s^2 + \frac{1}{2}\lambda_1 h_d^2 + \frac{1}{2}\lambda_3 h_u^2 & \frac{1}{\sqrt{2}}m_4 s - \frac{1}{2}\lambda_7 s^2 - \frac{1}{2}\lambda_4 h_d h_u \\ \dots & m_2^2 + \frac{1}{2}\lambda_6 s^2 + \frac{1}{2}\lambda_3 h_d^2 + \frac{1}{2}\lambda_2 h_u^2 \end{pmatrix}. \quad (\text{C.3})$$

The mass parameters m_1^2 , m_2^2 and m_3^2 are determined via the minimization conditions (the tadpoles) of $V_{\text{tree}}^{\text{THDMS}}$ of equation A.2 and are given by

$$\begin{aligned} m_1^2 &= -\frac{1}{2}(\lambda_3 + \lambda_4)v_u^2 - \frac{1}{2}\lambda_1 v_d^2 - \frac{1}{2}\lambda_5 v_s^2 - \frac{1}{2}\lambda_7 \frac{v_u v_s^2}{v_d} + \frac{1}{\sqrt{2}}m_4 \frac{v_u v_s}{v_d}, \\ m_2^2 &= -\frac{1}{2}\lambda_2 v_u^2 - \frac{1}{2}(\lambda_3 + \lambda_4)v_d^2 - \frac{1}{2}\lambda_6 v_s^2 - \frac{1}{2}\lambda_7 \frac{v_d v_s^2}{v_u} + \frac{1}{\sqrt{2}}m_4 \frac{v_d v_s}{v_u}, \\ m_3^2 &= -\frac{1}{2}\lambda_6 v_u^2 - \frac{1}{2}\lambda_5 v_d^2 - \lambda_8 v_s^2 - \lambda_7 v_d v_u + \frac{1}{\sqrt{2}}m_4 \frac{v_u v_d}{v_s} + \frac{1}{\sqrt{2}}m_5 v_s. \end{aligned} \quad (\text{C.4})$$

Diagonalization of \mathcal{M}_A^2 in equation C.2 leads to two neutral CP -odd scalars and a Goldstone boson. Similarly, diagonalization of $\mathcal{M}_{H^\pm}^2$ in equation C.3 results in a charged Higgs boson and a charged Goldstone boson. The masses of these neutral and charged Goldstone bosons are zero at the electroweak minima where the CP -even fields acquire values $\{v_d, v_u, v_s\}$. However, the gauge-fixing terms in the Lagrangian alter the tree-level mass matrices. In the Feynman gauge that we opt for this work, the mass matrices get modified and the

⁸Note that the NMSSM parameters are in the $\overline{\text{DR}}$ scheme [48] whereas, for the calculations of phase transitions, the THDMS parameters are provided in the $\overline{\text{MS}}$ scheme [37]. We ignore the effect of this shift in the scheme as this would modify the quartic couplings only mildly due to small threshold corrections. To convince ourselves, we have compared the mass-eigenvalues of the CP -even Higgs mass-squared matrix and the related mixing matrix that are obtained from `CosmoTransitions` to the corresponding ones obtained using `NMSSMTools` and their agreements are found to be within the level of a few percent.

Goldstone bosons no longer remain massless at the electroweak minima. We include these gauge-dependent contributions to \mathcal{M}_A^2 and $\mathcal{M}_{H^\pm}^2$ which are listed in reference [52].

Note that the one-loop CW potential (of equation 3.1) shifts the location of the electroweak minimum from where it was appearing in the field space for the tree-level potential. In the $\overline{\text{MS}}$ renormalization scheme that we adopt, one can find suitable counter-terms (as described in reference [108]) that modify the quadratic terms ($m_1^2 h_d^2 + m_2^2 h_u^2 + m_3^2 s^2$) in the potential (of equation A.2) thus ensuring the minimum of the effective potential coincides with that of the tree-level potential. The accompanying shifts in the mass parameters of the potential (obtained from equation C.4) are given by

$$m_1^2 \rightarrow m_1^2 - \frac{1}{v_d} \frac{\partial V_{\text{CW}}}{\partial h_d} \Big|_{\substack{h_d=v_d, \\ h_u=v_u, \\ s=v_s}}, \quad m_2^2 \rightarrow m_2^2 - \frac{1}{v_u} \frac{\partial V_{\text{CW}}}{\partial h_u} \Big|_{\substack{h_d=v_d, \\ h_u=v_u, \\ s=v_s}}, \quad m_3^2 \rightarrow m_3^2 - \frac{1}{v_s} \frac{\partial V_{\text{CW}}}{\partial s} \Big|_{\substack{h_d=v_d, \\ h_u=v_u, \\ s=v_s}}, \quad (\text{C.5})$$

Note that in the tree-level field-dependent mass-squared matrices (see equations C.1, C.2 and C.3) the values of m_1^2 , m_2^2 and m_3^2 are without this modification since the latter are solutions of the corresponding tree-level tadpole equations as presented in equation C.4.

In the fermionic sector, we consider the top quark, the bottom quark, the tau lepton along with the four neutralinos ($\chi_{1,2,3,4}^0$) and the one chargino (χ_1^\pm), since the wino-like states are taken to be much heavier and hence are decoupled from the physics of phase transitions. The field-dependent masses of the top quark, the bottom quark and the tau lepton are given by [48]

$$m_t = \frac{1}{\sqrt{2}} y_t h_u, \quad m_b = \frac{1}{\sqrt{2}} y_b h_d, \quad m_\tau = \frac{1}{\sqrt{2}} y_\tau h_d. \quad (\text{C.6})$$

The field-dependent 4×4 , symmetric neutralino mass matrix in the basis $\{\tilde{B}, \tilde{H}_d^0, \tilde{H}_u^0, \tilde{S}\}$ is given by

$$\mathcal{M}_{\chi^0} = \begin{pmatrix} M_1 - \frac{g_1 h_d}{2} & \frac{g_1 h_u}{2} & 0 \\ \dots & 0 & -\frac{\lambda s}{\sqrt{2}} \\ \dots & \dots & 0 \\ \dots & \dots & \dots \end{pmatrix}. \quad (\text{C.7})$$

On the other hand, the field-dependent mass of the higgsino-like chargino is given approximately by $m_{\chi_1^\pm} \simeq \frac{\lambda s}{\sqrt{2}}$. Note that the masses of these electroweakinos are given in terms of the NMSSM model parameters which are defined at the scale M_{SUSY} . This is acceptable for our purpose since these masses do not appear in the tree-level potential.⁹

The field-dependent masses of the gauge bosons, W^\pm and Z , are given by

$$m_{W^\pm}^2 = \frac{1}{4} g_2^2 (h_u^2 + h_d^2), \quad m_Z^2 = \frac{1}{4} (g_1^2 + g_2^2) (h_u^2 + h_d^2). \quad (\text{C.8})$$

Note that in the daisy potential of equation 3.6, M_h^2 and M_V^2 are the eigenvalues of the thermally improved (i.e., Debye-corrected) mass-squared matrices for the Higgs and the gauge bosons, respectively, i.e., generically, $M^2 = \text{eigenvalues}[\mathcal{M}^2 + \Delta(T^2)]$ where $\Delta(T^2) = c_{ij} T^2$ and c_{ij} 's are the so-called daisy coefficients. From the high temperature expansion of the

⁹The electroweakino masses, however, contribute to higher-order (starting at one-loop) corrections to the tree-level potential. Thus, the consideration of running of these masses amounts to having an even higher-order correction to the potential. Hence we ignore such a running.

thermal one-loop potential \tilde{V}_T (of equation 3.3) using equation 3.5, the daisy coefficients can be found from the following relation:

$$c_{ij} = \frac{1}{T^2} \frac{\partial^2 \tilde{V}_T}{\partial \phi_i \partial \phi_j} \Big|_{T^2 \gg m^2}. \quad (\text{C.9})$$

For an FOPT, the daisy correction is especially important since it has an impact on the all very critical cubic term of the potential at a finite temperature. Effects of only the scalars and the longitudinal modes of the vectors are included in this contribution. Thermal contributions to the transverse modes are suppressed due to gauge symmetry [210]. With these in mind, the various daisy coefficients (neglecting the electroweakino contributions) are as follows [52, 95, 211, 212]:

$$c_{11}^H = c_{11}^A = c_{11}^{H^\pm} = \frac{1}{24} \left(6\lambda_2 + 4\lambda_3 + 2\lambda_4 + 2\lambda_6 + 6y_t^2 + \frac{3}{2}g_1^2 + \frac{9}{2}g_2^2 \right), \quad (\text{C.10a})$$

$$c_{22}^H = c_{22}^A = c_{22}^{H^\pm} = \frac{1}{24} \left(6\lambda_1 + 4\lambda_3 + 2\lambda_4 + 2\lambda_5 + 6y_b^2 + 2y_\tau^2 + \frac{3}{2}g_1^2 + \frac{9}{2}g_2^2 \right), \quad (\text{C.10b})$$

$$c_{33}^H = c_{33}^A = \frac{1}{24} (4\lambda_5 + 4\lambda_6 + 8\lambda_8), \quad (\text{C.10c})$$

where the subscripts $\{1, 2, 3\}$ refer to the fields $\{h_d, h_u, s\}$. Note that the gauge symmetries plus the discrete Z_3 symmetry of the model set the off-diagonal terms of the $\Delta(T^2)$ matrix to zero (i.e. $\Delta(T^2)$ is a diagonal matrix). The longitudinal components of the gauge bosons receive thermal corrections. For W^\pm bosons the correction is $c_L^{W^\pm} = 2g_2^2 T^2$. Thus, the thermally improved mass of the longitudinally polarized W^\pm bosons is given by

$$M_{W_L^\pm}^2 = \frac{1}{4} g_2^2 (h_d^2 + h_u^2) + 2g_2^2 T^2. \quad (\text{C.11})$$

Similarly, the longitudinal components of the Z -boson and the photon (A) fields also receive thermal corrections. Their masses can be determined by diagonalizing the following matrix:

$$\frac{1}{4} (h_d^2 + h_u^2) \begin{pmatrix} g_2^2 & -g_2 g_1 \\ -g_1 g_2 & g_1^2 \end{pmatrix} + \begin{pmatrix} 2g_2^2 T^2 & 0 \\ 0 & 2g_1^2 T^2 \end{pmatrix}. \quad (\text{C.12})$$

The thermally improved masses of the longitudinally polarized Z -boson and the photon are given by

$$M_{Z_L, \gamma_L}^2 = \frac{1}{8} (g_2^2 + g_1^2) (h_d^2 + h_u^2) + (g_2^2 + g_1^2) T^2 \pm \delta, \quad (\text{C.13})$$

where

$$\delta = \sqrt{\frac{1}{64} (g_2^2 + g_1^2)^2 (h_d^2 + h_u^2 + 8T^2)^2 - g_2^2 g_1^2 T^2 (h_d^2 + h_u^2 + 4T^2)}. \quad (\text{C.14})$$

References

- [1] V. A. Kuzmin, V. A. Rubakov and M. E. Shaposhnikov, Phys. Lett. B **155** (1985), 36 doi:10.1016/0370-2693(85)91028-7
- [2] M. E. Shaposhnikov, JETP Lett. **44** (1986), 465-468
- [3] M. E. Shaposhnikov, Nucl. Phys. B **287** (1987), 757-775 doi:10.1016/0550-3213(87)90127-1

- [4] P. A. R. Ade *et al.* [Planck], *Astron. Astrophys.* **594** (2016), A13
doi:10.1051/0004-6361/201525830 [arXiv:1502.01589 [astro-ph.CO]].
- [5] A. D. Sakharov, *Pisma Zh. Eksp. Teor. Fiz.* **5** (1967), 32-35
doi:10.1070/PU1991v034n05ABEH002497
- [6] H. Georgi and S. L. Glashow, *Phys. Rev. Lett.* **32** (1974), 438-441
doi:10.1103/PhysRevLett.32.438
- [7] E. W. Kolb and M. S. Turner, *Front. Phys.* **69** (1990), 1-547 doi:10.1201/9780429492860
- [8] A. G. Cohen, D. B. Kaplan and A. E. Nelson, *Ann. Rev. Nucl. Part. Sci.* **43** (1993), 27-70
doi:10.1146/annurev.ns.43.120193.000331 [arXiv:hep-ph/9302210 [hep-ph]].
- [9] M. Fukugita and T. Yanagida, *Phys. Lett. B* **174** (1986), 45-47
doi:10.1016/0370-2693(86)91126-3
- [10] G. D'Ambrosio, G. F. Giudice and M. Raidal, *Phys. Lett. B* **575** (2003), 75-84
doi:10.1016/j.physletb.2003.09.037 [arXiv:hep-ph/0308031 [hep-ph]].
- [11] A. Pilaftsis and T. E. J. Underwood, *Nucl. Phys. B* **692** (2004), 303-345
doi:10.1016/j.nuclphysb.2004.05.029 [arXiv:hep-ph/0309342 [hep-ph]].
- [12] I. Affleck and M. Dine, *Nucl. Phys. B* **249** (1985), 361-380 doi:10.1016/0550-3213(85)90021-5
- [13] M. Dine, L. Randall and S. D. Thomas, *Nucl. Phys. B* **458** (1996), 291-326
doi:10.1016/0550-3213(95)00538-2 [arXiv:hep-ph/9507453 [hep-ph]].
- [14] H. Davoudiasl, R. Kitano, G. D. Kribs, H. Murayama and P. J. Steinhardt, *Phys. Rev. Lett.* **93** (2004), 201301 doi:10.1103/PhysRevLett.93.201301 [arXiv:hep-ph/0403019 [hep-ph]].
- [15] V. A. Rubakov and M. E. Shaposhnikov, *Usp. Fiz. Nauk* **166** (1996), 493-537
doi:10.1070/PU1996v039n05ABEH000145 [arXiv:hep-ph/9603208 [hep-ph]].
- [16] M. Trodden, *Rev. Mod. Phys.* **71** (1999), 1463-1500 doi:10.1103/RevModPhys.71.1463
[arXiv:hep-ph/9803479 [hep-ph]].
- [17] A. Riotto, [arXiv:hep-ph/9807454 [hep-ph]].
- [18] J. M. Cline, [arXiv:hep-ph/0609145 [hep-ph]].
- [19] D. E. Morrissey and M. J. Ramsey-Musolf, *New J. Phys.* **14** (2012), 125003
doi:10.1088/1367-2630/14/12/125003 [arXiv:1206.2942 [hep-ph]].
- [20] G. A. White, doi:10.1088/978-1-6817-4457-5
- [21] G. 't Hooft, *Phys. Rev. Lett.* **37** (1976), 8-11 doi:10.1103/PhysRevLett.37.8
- [22] G. Aad *et al.* [ATLAS], *Phys. Lett. B* **716** (2012), 1-29 doi:10.1016/j.physletb.2012.08.020
[arXiv:1207.7214 [hep-ex]].
- [23] S. Chatrchyan *et al.* [CMS], *Phys. Lett. B* **716** (2012), 30-61 doi:10.1016/j.physletb.2012.08.021
[arXiv:1207.7235 [hep-ex]].
- [24] A. I. Bochkarev and M. E. Shaposhnikov, *Mod. Phys. Lett. A* **2** (1987), 417
doi:10.1142/S0217732387000537
- [25] K. Kajantie, M. Laine, K. Rummukainen and M. E. Shaposhnikov, *Nucl. Phys. B* **466** (1996), 189-258 doi:10.1016/0550-3213(96)00052-1 [arXiv:hep-lat/9510020 [hep-lat]].

- [26] M. B. Gavela, P. Hernandez, J. Orloff and O. Pene, *Mod. Phys. Lett. A* **9** (1994), 795-810 doi:10.1142/S0217732394000629 [arXiv:hep-ph/9312215 [hep-ph]].
- [27] P. Huet and E. Sather, *Phys. Rev. D* **51** (1995), 379-394 doi:10.1103/PhysRevD.51.379 [arXiv:hep-ph/9404302 [hep-ph]].
- [28] M. B. Gavela, P. Hernandez, J. Orloff, O. Pene and C. Quimbay, *Nucl. Phys. B* **430** (1994), 382-426 doi:10.1016/0550-3213(94)00410-2 [arXiv:hep-ph/9406289 [hep-ph]].
- [29] J. I. Kapusta and C. Gale, doi:10.1017/CBO9780511535130
- [30] J. R. Espinosa, M. Quiros and F. Zwirner, *Phys. Lett. B* **307** (1993), 106-115 doi:10.1016/0370-2693(93)90199-R [arXiv:hep-ph/9303317 [hep-ph]].
- [31] M. Pietroni, *Nucl. Phys. B* **402** (1993), 27-45 doi:10.1016/0550-3213(93)90635-3 [arXiv:hep-ph/9207227 [hep-ph]].
- [32] S. Liebler, S. Profumo and T. Stefaniak, *JHEP* **04** (2016), 143 doi:10.1007/JHEP04(2016)143 [arXiv:1512.09172 [hep-ph]].
- [33] M. Carena, N. R. Shah and C. E. M. Wagner, *Phys. Rev. D* **85** (2012), 036003 doi:10.1103/PhysRevD.85.036003 [arXiv:1110.4378 [hep-ph]].
- [34] J. Kozaczuk, S. Profumo and C. L. Wainwright, *Phys. Rev. D* **87** (2013) no.7, 075011 doi:10.1103/PhysRevD.87.075011 [arXiv:1302.4781 [hep-ph]].
- [35] W. Huang, Z. Kang, J. Shu, P. Wu and J. M. Yang, *Phys. Rev. D* **91** (2015) no.2, 025006 doi:10.1103/PhysRevD.91.025006 [arXiv:1405.1152 [hep-ph]].
- [36] X. J. Bi, L. Bian, W. Huang, J. Shu and P. F. Yin, *Phys. Rev. D* **92** (2015), 023507 doi:10.1103/PhysRevD.92.023507 [arXiv:1503.03749 [hep-ph]].
- [37] J. Kozaczuk, S. Profumo, L. S. Haskins and C. L. Wainwright, *JHEP* **01** (2015), 144 doi:10.1007/JHEP01(2015)144 [arXiv:1407.4134 [hep-ph]].
- [38] L. Bian, H. K. Guo and J. Shu, *Chin. Phys. C* **42** (2018) no.9, 093106 [erratum: *Chin. Phys. C* **43** (2019) no.12, 129101] doi:10.1088/1674-1137/42/9/093106 [arXiv:1704.02488 [hep-ph]].
- [39] S. J. Huber, T. Konstandin, T. Prokopec and M. G. Schmidt, *Nucl. Phys. B* **757** (2006), 172-196 doi:10.1016/j.nuclphysb.2006.09.003 [arXiv:hep-ph/0606298 [hep-ph]].
- [40] C. Balázs, A. Mazumdar, E. Pukartas and G. White, *JHEP* **01** (2014), 073 doi:10.1007/JHEP01(2014)073 [arXiv:1309.5091 [hep-ph]].
- [41] K. Cheung, T. J. Hou, J. S. Lee and E. Senaha, *Phys. Lett. B* **710** (2012), 188-191 doi:10.1016/j.physletb.2012.02.070 [arXiv:1201.3781 [hep-ph]].
- [42] A. T. Davies, C. D. Froggatt and R. G. Moorhouse, *Phys. Lett. B* **372** (1996), 88-94 doi:10.1016/0370-2693(96)00076-7 [arXiv:hep-ph/9603388 [hep-ph]].
- [43] A. Menon, D. E. Morrissey and C. E. M. Wagner, *Phys. Rev. D* **70** (2004), 035005 doi:10.1103/PhysRevD.70.035005 [arXiv:hep-ph/0404184 [hep-ph]].
- [44] K. Funakubo, S. Tao and F. Toyoda, *Prog. Theor. Phys.* **114** (2005), 369-389 doi:10.1143/PTP.114.369 [arXiv:hep-ph/0501052 [hep-ph]].
- [45] S. J. Huber and T. Konstandin, *JCAP* **05** (2008), 017 doi:10.1088/1475-7516/2008/05/017 [arXiv:0709.2091 [hep-ph]].

- [46] J. R. Espinosa, T. Konstandin and F. Riva, Nucl. Phys. B **854** (2012), 592-630
doi:10.1016/j.nuclphysb.2011.09.010 [arXiv:1107.5441 [hep-ph]].
- [47] S. J. Huber, T. Konstandin, G. Nardini and I. Rues, JCAP **03** (2016), 036
doi:10.1088/1475-7516/2016/03/036 [arXiv:1512.06357 [hep-ph]].
- [48] U. Ellwanger, C. Hugonie and A. M. Teixeira, Phys. Rept. **496** (2010), 1-77
doi:10.1016/j.physrep.2010.07.001 [arXiv:0910.1785 [hep-ph]].
- [49] S. V. Demidov, D. S. Gorbunov and D. V. Kirpichnikov, JHEP **11** (2016), 148 [erratum: JHEP **08** (2017), 080] doi:10.1007/JHEP11(2016)148 [arXiv:1608.01985 [hep-ph]].
- [50] S. Akula, C. Balázs, L. Dunn and G. White, JHEP **11** (2017), 051
doi:10.1007/JHEP11(2017)051 [arXiv:1706.09898 [hep-ph]].
- [51] S. V. Demidov, D. S. Gorbunov and D. V. Kirpichnikov, Phys. Lett. B **779** (2018), 191-194
doi:10.1016/j.physletb.2018.02.007 [arXiv:1712.00087 [hep-ph]].
- [52] P. Athron, C. Balázs, A. Fowlie, G. Pozzo, G. White and Y. Zhang, JHEP **11** (2019), 151
doi:10.1007/JHEP11(2019)151 [arXiv:1908.11847 [hep-ph]].
- [53] P. Athron, C. Balázs, A. Fowlie and Y. Zhang, Eur. Phys. J. C **80** (2020) no.6, 567
doi:10.1140/epjc/s10052-020-8035-2 [arXiv:2003.02859 [hep-ph]].
- [54] S. Baum, M. Carena, N. R. Shah, C. E. M. Wagner and Y. Wang, JHEP **03** (2021), 055
doi:10.1007/JHEP03(2021)055 [arXiv:2009.10743 [hep-ph]].
- [55] C. L. Wainwright, Comput. Phys. Commun. **183** (2012), 2006-2013
doi:10.1016/j.cpc.2012.04.004 [arXiv:1109.4189 [hep-ph]].
- [56] E. Witten, Phys. Rev. D **30** (1984), 272-285 doi:10.1103/PhysRevD.30.272
- [57] C. J. Hogan, Mon. Not. Roy. Astron. Soc. **218** (1986), 629-636
- [58] R. Apreda, M. Maggiore, A. Nicolis and A. Riotto, Nucl. Phys. B **631** (2002), 342-368
doi:10.1016/S0550-3213(02)00264-X [arXiv:gr-qc/0107033 [gr-qc]].
- [59] C. Grojean, G. Servant and J. D. Wells, Phys. Rev. D **71** (2005), 036001
doi:10.1103/PhysRevD.71.036001 [arXiv:hep-ph/0407019 [hep-ph]].
- [60] D. J. Weir, Phil. Trans. Roy. Soc. Lond. A **376** (2018) no.2114, 20170126
doi:10.1098/rsta.2017.0126 [arXiv:1705.01783 [hep-ph]].
- [61] J. Ellis, M. Lewicki and J. M. No, JCAP **04** (2019), 003 doi:10.1088/1475-7516/2019/04/003
[arXiv:1809.08242 [hep-ph]].
- [62] T. Alanne, T. Hügler, M. Platscher and K. Schmitz, JHEP **03** (2020), 004
doi:10.1007/JHEP03(2020)004 [arXiv:1909.11356 [hep-ph]].
- [63] C. Caprini, M. Chala, G. C. Dorsch, M. Hindmarsh, S. J. Huber, T. Konstandin, J. Kozaczuk,
G. Nardini, J. M. No and K. Rummukainen, *et al.* JCAP **03** (2020), 024
doi:10.1088/1475-7516/2020/03/024 [arXiv:1910.13125 [astro-ph.CO]].
- [64] S. R. Coleman and E. J. Weinberg, Phys. Rev. D **7** (1973), 1888-1910
doi:10.1103/PhysRevD.7.1888
- [65] L. Dolan and R. Jackiw, Phys. Rev. D **9** (1974), 3320-3341 doi:10.1103/PhysRevD.9.3320
- [66] S. Weinberg, Phys. Rev. D **9** (1974), 3357-3378 doi:10.1103/PhysRevD.9.3357

- [67] A. D. Linde, Phys. Lett. B **70** (1977), 306-308 doi:10.1016/0370-2693(77)90664-5
- [68] A. D. Linde, Rept. Prog. Phys. **42** (1979), 389 doi:10.1088/0034-4885/42/3/001
- [69] A. D. Linde, Nucl. Phys. B **216** (1983), 421 [erratum: Nucl. Phys. B **223** (1983), 544] doi:10.1016/0550-3213(83)90072-X
- [70] J. S. Langer, Annals Phys. **54** (1969), 258-275 doi:10.1016/0003-4916(69)90153-5
- [71] S. R. Coleman, Phys. Rev. D **15** (1977), 2929-2936 [erratum: Phys. Rev. D **16** (1977), 1248] doi:10.1103/PhysRevD.16.1248
- [72] I. Affleck, Phys. Rev. Lett. **46** (1981), 388 doi:10.1103/PhysRevLett.46.388
- [73] M. Quiros, [arXiv:hep-ph/9901312 [hep-ph]].
- [74] A. Mazumdar and G. White, Rept. Prog. Phys. **82** (2019) no.7, 076901 doi:10.1088/1361-6633/ab1f55 [arXiv:1811.01948 [hep-ph]].
- [75] S. L. Adler, Phys. Rev. **177** (1969), 2426-2438 doi:10.1103/PhysRev.177.2426
- [76] J. S. Bell and R. Jackiw, Nuovo Cim. A **60** (1969), 47-61 doi:10.1007/BF02823296
- [77] N. S. Manton, Phys. Rev. D **28** (1983), 2019 doi:10.1103/PhysRevD.28.2019
- [78] F. R. Klinkhamer and N. S. Manton, Phys. Rev. D **30** (1984), 2212 doi:10.1103/PhysRevD.30.2212
- [79] J. Kunz, B. Kleihaus and Y. Brihaye, Phys. Rev. D **46** (1992), 3587-3600 doi:10.1103/PhysRevD.46.3587
- [80] P. B. Arnold and L. D. McLerran, Phys. Rev. D **36** (1987), 581 doi:10.1103/PhysRevD.36.581
- [81] S. Y. Khlebnikov and M. E. Shaposhnikov, Nucl. Phys. B **308** (1988), 885-912 doi:10.1016/0550-3213(88)90133-2
- [82] L. Carson, X. Li, L. D. McLerran and R. T. Wang, Phys. Rev. D **42** (1990), 2127-2143 doi:10.1103/PhysRevD.42.2127
- [83] J. M. Moreno, D. H. Oaknin and M. Quiros, Nucl. Phys. B **483** (1997), 267-290 doi:10.1016/S0550-3213(96)00562-7 [arXiv:hep-ph/9605387 [hep-ph]].
- [84] K. Funakubo, A. Kakuto, S. Tao and F. Toyoda, Prog. Theor. Phys. **114** (2006), 1069-1082 doi:10.1143/PTP.114.1069 [arXiv:hep-ph/0506156 [hep-ph]].
- [85] G. R. Farrar and M. E. Shaposhnikov, Phys. Rev. Lett. **70** (1993), 2833-2836 [erratum: Phys. Rev. Lett. **71** (1993), 210] doi:10.1103/PhysRevLett.70.2833 [arXiv:hep-ph/9305274 [hep-ph]].
- [86] G. R. Farrar and M. E. Shaposhnikov, Phys. Rev. D **50** (1994), 774 doi:10.1103/PhysRevD.50.774 [arXiv:hep-ph/9305275 [hep-ph]].
- [87] D. Bodeker, G. D. Moore and K. Rummukainen, Phys. Rev. D **61** (2000), 056003 doi:10.1103/PhysRevD.61.056003 [arXiv:hep-ph/9907545 [hep-ph]].
- [88] A. I. Bochkaev, S. V. Kuzmin and M. E. Shaposhnikov, Phys. Rev. D **43** (1991), 369-374 doi:10.1103/PhysRevD.43.369
- [89] G. D. Moore, Phys. Rev. D **59** (1999), 014503 doi:10.1103/PhysRevD.59.014503 [arXiv:hep-ph/9805264 [hep-ph]].
- [90] H. H. Patel and M. J. Ramsey-Musolf, JHEP **07** (2011), 029 doi:10.1007/JHEP07(2011)029 [arXiv:1101.4665 [hep-ph]].

- [91] D. A. Kirzhnits and A. D. Linde, *Annals Phys.* **101** (1976), 195-238
doi:10.1016/0003-4916(76)90279-7
- [92] G. W. Anderson and L. J. Hall, *Phys. Rev. D* **45** (1992), 2685-2698
doi:10.1103/PhysRevD.45.2685
- [93] P. B. Arnold and O. Espinosa, *Phys. Rev. D* **47** (1993), 3546 [erratum: *Phys. Rev. D* **50** (1994), 6662] doi:10.1103/PhysRevD.47.3546 [arXiv:hep-ph/9212235 [hep-ph]].
- [94] R. R. Parwani, *Phys. Rev. D* **45** (1992), 4695 [erratum: *Phys. Rev. D* **48** (1993), 5965] doi:10.1103/PhysRevD.45.4695 [arXiv:hep-ph/9204216 [hep-ph]].
- [95] M. E. Carrington, *Phys. Rev. D* **45** (1992), 2933-2944 doi:10.1103/PhysRevD.45.2933
- [96] N. K. Nielsen, *Nucl. Phys. B* **101** (1975), 173-188 doi:10.1016/0550-3213(75)90301-6
- [97] R. Fukuda and T. Kugo, *Phys. Rev. D* **13** (1976), 3469 doi:10.1103/PhysRevD.13.3469
- [98] M. Laine, *Phys. Rev. D* **51** (1995), 4525-4532 doi:10.1103/PhysRevD.51.4525 [arXiv:hep-ph/9411252 [hep-ph]].
- [99] J. Baacke and S. Junker, *Phys. Rev. D* **49** (1994), 2055-2073 doi:10.1103/PhysRevD.49.2055 [arXiv:hep-ph/9308310 [hep-ph]].
- [100] J. Baacke and S. Junker, *Phys. Rev. D* **50** (1994), 4227-4228 doi:10.1103/PhysRevD.50.4227 [arXiv:hep-th/9402078 [hep-th]].
- [101] M. Garny and T. Konstandin, *JHEP* **07** (2012), 189 doi:10.1007/JHEP07(2012)189 [arXiv:1205.3392 [hep-ph]].
- [102] J. R. Espinosa, M. Garny, T. Konstandin and A. Riotto, *Phys. Rev. D* **95** (2017) no.5, 056004 doi:10.1103/PhysRevD.95.056004 [arXiv:1608.06765 [hep-ph]].
- [103] S. Arunasalam and M. J. Ramsey-Musolf, [arXiv:2105.07588 [hep-ph]].
- [104] J. Löfgren, M. J. Ramsey-Musolf, P. Schicho and T. V. I. Tenkanen, [arXiv:2112.05472 [hep-ph]].
- [105] T. Elliott, S. F. King and P. L. White, *Phys. Lett. B* **305** (1993), 71-77 doi:10.1016/0370-2693(93)91107-X [arXiv:hep-ph/9302202 [hep-ph]].
- [106] T. Elliott, S. F. King and P. L. White, *Phys. Lett. B* **314** (1993), 56-63 doi:10.1016/0370-2693(93)91321-D [arXiv:hep-ph/9305282 [hep-ph]].
- [107] T. Elliott, S. F. King and P. L. White, *Phys. Rev. D* **49** (1994), 2435-2456 doi:10.1103/PhysRevD.49.2435 [arXiv:hep-ph/9308309 [hep-ph]].
- [108] J. M. Cline, K. Kainulainen and M. Trott, *JHEP* **11** (2011), 089 doi:10.1007/JHEP11(2011)089 [arXiv:1107.3559 [hep-ph]].
- [109] M. Badziak, M. Olechowski and P. Szczerbiak, *JHEP* **03** (2016), 179 doi:10.1007/JHEP03(2016)179 [arXiv:1512.02472 [hep-ph]].
- [110] C. Cheung, L. J. Hall, D. Pinner and J. T. Ruderman, *JHEP* **05** (2013), 100 doi:10.1007/JHEP05(2013)100 [arXiv:1211.4873 [hep-ph]].
- [111] C. Cheung, M. Papucci, D. Sanford, N. R. Shah and K. M. Zurek, *Phys. Rev. D* **90** (2014) no.7, 075011 doi:10.1103/PhysRevD.90.075011 [arXiv:1406.6372 [hep-ph]].

- [112] M. Badziak, M. Olechowski and P. Szczerbiak, PoS **PLANCK2015** (2015), 130 [arXiv:1601.00768 [hep-ph]].
- [113] M. Badziak, M. Olechowski and P. Szczerbiak, JHEP **07** (2017), 050 doi:10.1007/JHEP07(2017)050 [arXiv:1705.00227 [hep-ph]].
- [114] M. Aaboud *et al.* [ATLAS], JHEP **06** (2018), 166 doi:10.1007/JHEP06(2018)166 [arXiv:1802.03388 [hep-ex]].
- [115] M. Aaboud *et al.* [ATLAS], Phys. Lett. B **782** (2018), 750-767 doi:10.1016/j.physletb.2018.06.011 [arXiv:1803.11145 [hep-ex]].
- [116] A. M. Sirunyan *et al.* [CMS], JHEP **08** (2020), 139 doi:10.1007/JHEP08(2020)139 [arXiv:2005.08694 [hep-ex]].
- [117] G. Aad *et al.* [ATLAS], Phys. Rev. D **105** (2022) no.1, 012006 doi:10.1103/PhysRevD.105.012006 [arXiv:2110.00313 [hep-ex]].
- [118] J. R. Ellis, K. Enqvist, D. V. Nanopoulos and F. Zwirner, Mod. Phys. Lett. A **1** (1986), 57 doi:10.1142/S0217732386000105
- [119] R. Barbieri and G. F. Giudice, Nucl. Phys. B **306** (1988), 63-76 doi:10.1016/0550-3213(88)90171-X
- [120] H. Baer, V. Barger, P. Huang, A. Mustafayev and X. Tata, Phys. Rev. Lett. **109** (2012), 161802 doi:10.1103/PhysRevLett.109.161802 [arXiv:1207.3343 [hep-ph]].
- [121] H. Baer, V. Barger, P. Huang, D. Mickelson, A. Mustafayev and X. Tata, Phys. Rev. D **87** (2013) no.11, 115028 doi:10.1103/PhysRevD.87.115028 [arXiv:1212.2655 [hep-ph]].
- [122] W. Abdallah, A. Datta and S. Roy, JHEP **04** (2021), 122 doi:10.1007/JHEP04(2021)122 [arXiv:2012.04026 [hep-ph]].
- [123] G. Aad *et al.* [ATLAS], JHEP **06** (2021), 145 doi:10.1007/JHEP06(2021)145 [arXiv:2102.10076 [hep-ex]].
- [124] G. Aad *et al.* [ATLAS], Phys. Rev. Lett. **125** (2020) no.5, 051801 doi:10.1103/PhysRevLett.125.051801 [arXiv:2002.12223 [hep-ex]].
- [125] G. Aad *et al.* [ATLAS], Eur. Phys. J. C **81** (2021), 1118 doi:10.1140/epjc/s10052-021-09749-7 [arXiv:2106.01676 [hep-ex]].
- [126] A. Tumasyan *et al.* [CMS], [arXiv:2111.06296 [hep-ex]].
- [127] C. Caprini, M. Hindmarsh, S. Huber, T. Konstandin, J. Kozaczuk, G. Nardini, J. M. No, A. Petiteau, P. Schwaller and G. Servant, *et al.* JCAP **04** (2016), 001 doi:10.1088/1475-7516/2016/04/001 [arXiv:1512.06239 [astro-ph.CO]].
- [128] J. D. Romano and N. J. Cornish, Living Rev. Rel. **20** (2017) no.1, 2 doi:10.1007/s41114-017-0004-1 [arXiv:1608.06889 [gr-qc]].
- [129] R. G. Cai, Z. Cao, Z. K. Guo, S. J. Wang and T. Yang, Natl. Sci. Rev. **4** (2017) no.5, 687-706 doi:10.1093/nsr/nwx029 [arXiv:1703.00187 [gr-qc]].
- [130] C. Caprini and D. G. Figueroa, Class. Quant. Grav. **35** (2018) no.16, 163001 doi:10.1088/1361-6382/aac608 [arXiv:1801.04268 [astro-ph.CO]].
- [131] N. Christensen, Rept. Prog. Phys. **82** (2019) no.1, 016903 doi:10.1088/1361-6633/aae6b5 [arXiv:1811.08797 [gr-qc]].

- [132] A. Kosowsky, M. S. Turner and R. Watkins, Phys. Rev. D **45** (1992), 4514-4535
doi:10.1103/PhysRevD.45.4514
- [133] A. Kosowsky, M. S. Turner and R. Watkins, Phys. Rev. Lett. **69** (1992), 2026-2029
doi:10.1103/PhysRevLett.69.2026
- [134] A. Kosowsky and M. S. Turner, Phys. Rev. D **47** (1993), 4372-4391
doi:10.1103/PhysRevD.47.4372 [arXiv:astro-ph/9211004 [astro-ph]].
- [135] M. Kamionkowski, A. Kosowsky and M. S. Turner, Phys. Rev. D **49** (1994), 2837-2851
doi:10.1103/PhysRevD.49.2837 [arXiv:astro-ph/9310044 [astro-ph]].
- [136] C. Caprini, R. Durrer and G. Servant, Phys. Rev. D **77** (2008), 124015
doi:10.1103/PhysRevD.77.124015 [arXiv:0711.2593 [astro-ph]].
- [137] S. J. Huber and T. Konstandin, JCAP **09** (2008), 022 doi:10.1088/1475-7516/2008/09/022
[arXiv:0806.1828 [hep-ph]].
- [138] D. Bodeker and G. D. Moore, JCAP **05** (2017), 025 doi:10.1088/1475-7516/2017/05/025
[arXiv:1703.08215 [hep-ph]].
- [139] M. Hindmarsh, S. J. Huber, K. Rummukainen and D. J. Weir, Phys. Rev. Lett. **112** (2014),
041301 doi:10.1103/PhysRevLett.112.041301 [arXiv:1304.2433 [hep-ph]].
- [140] J. T. Giblin, Jr. and J. B. Mertens, JHEP **12** (2013), 042 doi:10.1007/JHEP12(2013)042
[arXiv:1310.2948 [hep-th]].
- [141] J. T. Giblin and J. B. Mertens, Phys. Rev. D **90** (2014) no.2, 023532
doi:10.1103/PhysRevD.90.023532 [arXiv:1405.4005 [astro-ph.CO]].
- [142] M. Hindmarsh, S. J. Huber, K. Rummukainen and D. J. Weir, Phys. Rev. D **92** (2015) no.12,
123009 doi:10.1103/PhysRevD.92.123009 [arXiv:1504.03291 [astro-ph.CO]].
- [143] T. M. C. Abbott *et al.* [DES], Mon. Not. Roy. Astron. Soc. **480** (2018) no.3, 3879-3888
doi:10.1093/mnras/sty1939 [arXiv:1711.00403 [astro-ph.CO]].
- [144] C. Caprini and R. Durrer, Phys. Rev. D **74** (2006), 063521 doi:10.1103/PhysRevD.74.063521
[arXiv:astro-ph/0603476 [astro-ph]].
- [145] T. Kahniashvili, A. Kosowsky, G. Gogoberidze and Y. Maravin, Phys. Rev. D **78** (2008),
043003 doi:10.1103/PhysRevD.78.043003 [arXiv:0806.0293 [astro-ph]].
- [146] T. Kahniashvili, L. Campanelli, G. Gogoberidze, Y. Maravin and B. Ratra, Phys. Rev. D **78**
(2008), 123006 [erratum: Phys. Rev. D **79** (2009), 109901] doi:10.1103/PhysRevD.78.123006
[arXiv:0809.1899 [astro-ph]].
- [147] T. Kahniashvili, L. Kisslinger and T. Stevens, Phys. Rev. D **81** (2010), 023004
doi:10.1103/PhysRevD.81.023004 [arXiv:0905.0643 [astro-ph.CO]].
- [148] C. Caprini, R. Durrer and G. Servant, JCAP **12** (2009), 024
doi:10.1088/1475-7516/2009/12/024 [arXiv:0909.0622 [astro-ph.CO]].
- [149] L. Kisslinger and T. Kahniashvili, Phys. Rev. D **92** (2015) no.4, 043006
doi:10.1103/PhysRevD.92.043006 [arXiv:1505.03680 [astro-ph.CO]].
- [150] J. R. Espinosa, T. Konstandin, J. M. No and G. Servant, JCAP **06** (2010), 028
doi:10.1088/1475-7516/2010/06/028 [arXiv:1004.4187 [hep-ph]].

- [151] M. Hindmarsh, Phys. Rev. Lett. **120** (2018) no.7, 071301 doi:10.1103/PhysRevLett.120.071301 [arXiv:1608.04735 [astro-ph.CO]].
- [152] M. Hindmarsh, S. J. Huber, K. Rummukainen and D. J. Weir, Phys. Rev. D **96** (2017) no.10, 103520 [erratum: Phys. Rev. D **101** (2020) no.8, 089902] doi:10.1103/PhysRevD.96.103520 [arXiv:1704.05871 [astro-ph.CO]].
- [153] C. W. Chiang and B. Q. Lu, JHEP **07** (2020), 082 doi:10.1007/JHEP07(2020)082 [arXiv:1912.12634 [hep-ph]].
- [154] H. K. Guo, K. Sinha, D. Vagie and G. White, JCAP **01** (2021), 001 doi:10.1088/1475-7516/2021/01/001 [arXiv:2007.08537 [hep-ph]].
- [155] M. B. Hindmarsh, M. Lüben, J. Lumma and M. Pauly, SciPost Phys. Lect. Notes **24** (2021), 1 doi:10.21468/SciPostPhysLectNotes.24 [arXiv:2008.09136 [astro-ph.CO]].
- [156] U. L. Pen and N. Turok, Phys. Rev. Lett. **117** (2016) no.13, 131301 doi:10.1103/PhysRevLett.117.131301 [arXiv:1510.02985 [astro-ph.CO]].
- [157] M. Hindmarsh and M. Hijazi, JCAP **12** (2019), 062 doi:10.1088/1475-7516/2019/12/062 [arXiv:1909.10040 [astro-ph.CO]].
- [158] J. M. No, Phys. Rev. D **84** (2011), 124025 doi:10.1103/PhysRevD.84.124025 [arXiv:1103.2159 [hep-ph]].
- [159] U. Ellwanger and C. Hugonie, Comput. Phys. Commun. **175** (2006), 290-303 doi:10.1016/j.cpc.2006.04.004 [arXiv:hep-ph/0508022 [hep-ph]].
- [160] D. Das, U. Ellwanger and A. M. Teixeira, Comput. Phys. Commun. **183** (2012), 774-779 doi:10.1016/j.cpc.2011.11.021 [arXiv:1106.5633 [hep-ph]].
- [161] P. Bechtle, D. Dercks, S. Heinemeyer, T. Klingl, T. Stefaniak, G. Weiglein and J. Wittbrodt, Eur. Phys. J. C **80** (2020) no.12, 1211 doi:10.1140/epjc/s10052-020-08557-9 [arXiv:2006.06007 [hep-ph]].
- [162] P. Bechtle, S. Heinemeyer, T. Klingl, T. Stefaniak, G. Weiglein and J. Wittbrodt, Eur. Phys. J. C **81** (2021) no.2, 145 doi:10.1140/epjc/s10052-021-08942-y [arXiv:2012.09197 [hep-ph]].
- [163] D. Dercks, N. Desai, J. S. Kim, K. Rolbiecki, J. Tattersall and T. Weber, Comput. Phys. Commun. **221** (2017), 383-418 doi:10.1016/j.cpc.2017.08.021 [arXiv:1611.09856 [hep-ph]].
- [164] G. Alguero, J. Heisig, C. Khosa, S. Kraml, S. Kulkarni, A. Lessa, H. Reyes-González, W. Waltenberger and A. Wongel, [arXiv:2112.00769 [hep-ph]].
- [165] A. M. Sirunyan *et al.* [CMS], JHEP **03** (2018), 160 doi:10.1007/JHEP03(2018)160 [arXiv:1801.03957 [hep-ex]].
- [166] A. M. Sirunyan *et al.* [CMS], Phys. Lett. B **782** (2018), 440-467 doi:10.1016/j.physletb.2018.05.062 [arXiv:1801.01846 [hep-ex]].
- [167] A. M. Sirunyan *et al.* [CMS], JHEP **03** (2018), 166 doi:10.1007/JHEP03(2018)166 [arXiv:1709.05406 [hep-ex]].
- [168] A. M. Sirunyan *et al.* [CMS], JHEP **11** (2018), 079 doi:10.1007/JHEP11(2018)079 [arXiv:1807.07799 [hep-ex]].
- [169] A. M. Sirunyan *et al.* [CMS], JHEP **11** (2017), 029 doi:10.1007/JHEP11(2017)029 [arXiv:1706.09933 [hep-ex]].

- [170] A. M. Sirunyan *et al.* [CMS], Phys. Lett. B **779** (2018), 166-190
doi:10.1016/j.physletb.2017.12.069 [arXiv:1709.00384 [hep-ex]].
- [171] A. M. Sirunyan *et al.* [CMS], JHEP **03** (2018), 076 doi:10.1007/s13130-018-7845-2
[arXiv:1709.08908 [hep-ex]].
- [172] M. Aaboud *et al.* [ATLAS], Phys. Rev. D **97** (2018) no.5, 052010
doi:10.1103/PhysRevD.97.052010 [arXiv:1712.08119 [hep-ex]].
- [173] M. Aaboud *et al.* [ATLAS], Eur. Phys. J. C **78** (2018) no.12, 995
doi:10.1140/epjc/s10052-018-6423-7 [arXiv:1803.02762 [hep-ex]].
- [174] M. Aaboud *et al.* [ATLAS], Phys. Rev. D **100** (2019) no.1, 012006
doi:10.1103/PhysRevD.100.012006 [arXiv:1812.09432 [hep-ex]].
- [175] M. Aaboud *et al.* [ATLAS], Phys. Rev. D **98** (2018) no.9, 092012
doi:10.1103/PhysRevD.98.092012 [arXiv:1806.02293 [hep-ex]].
- [176] G. Aad *et al.* [ATLAS], Eur. Phys. J. C **80** (2020) no.8, 691
doi:10.1140/epjc/s10052-020-8050-3 [arXiv:1909.09226 [hep-ex]].
- [177] G. Aad *et al.* [ATLAS], Phys. Rev. D **101** (2020) no.7, 072001
doi:10.1103/PhysRevD.101.072001 [arXiv:1912.08479 [hep-ex]].
- [178] G. Aad *et al.* [ATLAS], Eur. Phys. J. C **80** (2020) no.2, 123
doi:10.1140/epjc/s10052-019-7594-6 [arXiv:1908.08215 [hep-ex]].
- [179] G. Aad *et al.* [ATLAS], Phys. Rev. D **101** (2020) no.5, 052005
doi:10.1103/PhysRevD.101.052005 [arXiv:1911.12606 [hep-ex]].
- [180] G. Aad *et al.* [ATLAS], JHEP **10** (2020), 005 doi:10.1007/JHEP10(2020)005 [arXiv:2004.10894
[hep-ex]].
- [181] N. Aghanim *et al.* [Planck], Astron. Astrophys. **641** (2020), A6 [erratum: Astron. Astrophys.
652 (2021), C4] doi:10.1051/0004-6361/201833910 [arXiv:1807.06209 [astro-ph.CO]].
- [182] E. Aprile *et al.* [XENON], Phys. Rev. Lett. **121** (2018) no.11, 111302
doi:10.1103/PhysRevLett.121.111302 [arXiv:1805.12562 [astro-ph.CO]].
- [183] E. Aprile *et al.* [XENON], Phys. Rev. Lett. **122** (2019) no.14, 141301
doi:10.1103/PhysRevLett.122.141301 [arXiv:1902.03234 [astro-ph.CO]].
- [184] C. Amole *et al.* [PICO], Phys. Rev. D **100** (2019) no.2, 022001
doi:10.1103/PhysRevD.100.022001 [arXiv:1902.04031 [astro-ph.CO]].
- [185] G. Belanger, F. Boudjema, A. Pukhov and A. Semenov, Comput. Phys. Commun. **176** (2007),
367-382 doi:10.1016/j.cpc.2006.11.008 [arXiv:hep-ph/0607059 [hep-ph]].
- [186] A. Tumasyan *et al.* [CMS], [arXiv:2106.14246 [hep-ex]].
- [187] A. Tumasyan *et al.* [CMS], JHEP **10** (2021), 045 doi:10.1007/JHEP10(2021)045
[arXiv:2107.12553 [hep-ex]].
- [188] B. Abi *et al.* [Muon g-2], Phys. Rev. Lett. **126** (2021) no.14, 141801
doi:10.1103/PhysRevLett.126.141801 [arXiv:2104.03281 [hep-ex]].
- [189] G. W. Bennett *et al.* [Muon g-2], Phys. Rev. D **73** (2006), 072003
doi:10.1103/PhysRevD.73.072003 [arXiv:hep-ex/0602035 [hep-ex]].

- [190] J. Alwall, R. Frederix, S. Frixione, V. Hirschi, F. Maltoni, O. Mattelaer, H. S. Shao, T. Stelzer, P. Torrielli and M. Zaro, *JHEP* **07** (2014), 079 doi:10.1007/JHEP07(2014)079 [arXiv:1405.0301 [hep-ph]].
- [191] T. Sjöstrand, S. Ask, J. R. Christiansen, R. Corke, N. Desai, P. Ilten, S. Mrenna, S. Prestel, C. O. Rasmussen and P. Z. Skands, *Comput. Phys. Commun.* **191** (2015), 159-177 doi:10.1016/j.cpc.2015.01.024 [arXiv:1410.3012 [hep-ph]].
- [192] M. L. Mangano, M. Moretti, F. Piccinini and M. Treccani, *JHEP* **01** (2007), 013 doi:10.1088/1126-6708/2007/01/013 [arXiv:hep-ph/0611129 [hep-ph]].
- [193] J. de Favereau *et al.* [DELPHES 3], *JHEP* **02** (2014), 057 doi:10.1007/JHEP02(2014)057 [arXiv:1307.6346 [hep-ex]].
- [194] J. Fiaschi and M. Klasen, *Phys. Rev. D* **98** (2018) no.5, 055014 doi:10.1103/PhysRevD.98.055014 [arXiv:1805.11322 [hep-ph]].
- [195] U. Ellwanger and C. Hugonie, *Eur. Phys. J. C* **78** (2018) no.9, 735 doi:10.1140/epjc/s10052-018-6204-3 [arXiv:1806.09478 [hep-ph]].
- [196] F. Domingo, J. S. Kim, V. M. Lozano, P. Martin-Ramiro and R. Ruiz de Austri, *Phys. Rev. D* **101** (2020) no.7, 075010 doi:10.1103/PhysRevD.101.075010 [arXiv:1812.05186 [hep-ph]].
- [197] W. Abdallah, A. Chatterjee and A. Datta, *JHEP* **09** (2019), 095 doi:10.1007/JHEP09(2019)095 [arXiv:1907.06270 [hep-ph]].
- [198] J. Cao, Y. He, L. Shang, Y. Zhang and P. Zhu, *Phys. Rev. D* **99** (2019) no.7, 075020 doi:10.1103/PhysRevD.99.075020 [arXiv:1810.09143 [hep-ph]].
- [199] Private communications with J. Cao and D. Zhang.
- [200] P. Amaro-Seoane *et al.* [LISA], [arXiv:1702.00786 [astro-ph.IM]].
- [201] X. Gong, Y. K. Lau, S. Xu, P. Amaro-Seoane, S. Bai, X. Bian, Z. Cao, G. Chen, X. Chen and Y. Ding, *et al.* *J. Phys. Conf. Ser.* **610** (2015) no.1, 012011 doi:10.1088/1742-6596/610/1/012011 [arXiv:1410.7296 [gr-qc]].
- [202] J. Luo *et al.* [TianQin], *Class. Quant. Grav.* **33** (2016) no.3, 035010 doi:10.1088/0264-9381/33/3/035010 [arXiv:1512.02076 [astro-ph.IM]].
- [203] G. M. Harry [LIGO Scientific], *Class. Quant. Grav.* **27** (2010), 084006 doi:10.1088/0264-9381/27/8/084006
- [204] V. Corbin and N. J. Cornish, *Class. Quant. Grav.* **23** (2006), 2435-2446 doi:10.1088/0264-9381/23/7/014 [arXiv:gr-qc/0512039 [gr-qc]].
- [205] H. Kudoh, A. Taruya, T. Hiramatsu and Y. Himemoto, *Phys. Rev. D* **73** (2006), 064006 doi:10.1103/PhysRevD.73.064006 [arXiv:gr-qc/0511145 [gr-qc]].
- [206] J. R. Ellis, G. Ridolfi and F. Zwirner, *Phys. Lett. B* **262** (1991), 477-484 doi:10.1016/0370-2693(91)90626-2
- [207] H. E. Haber and R. Hempfling, *Phys. Rev. D* **48** (1993), 4280-4309 doi:10.1103/PhysRevD.48.4280 [arXiv:hep-ph/9307201 [hep-ph]].
- [208] J. A. Casas, J. R. Espinosa, M. Quiros and A. Riotto, *Nucl. Phys. B* **436** (1995), 3-29 [erratum: *Nucl. Phys. B* **439** (1995), 466-468] doi:10.1016/0550-3213(94)00508-C [arXiv:hep-ph/9407389 [hep-ph]].

- [209] M. Carena, J. R. Espinosa, M. Quiros and C. E. M. Wagner, Phys. Lett. B **355** (1995), 209-221 doi:10.1016/0370-2693(95)00694-G [arXiv:hep-ph/9504316 [hep-ph]].
- [210] J. R. Espinosa, M. Quiros and F. Zwirner, Phys. Lett. B **314** (1993), 206-216 doi:10.1016/0370-2693(93)90450-V [arXiv:hep-ph/9212248 [hep-ph]].
- [211] D. Comelli and J. R. Espinosa, Phys. Rev. D **55** (1997), 6253-6263 doi:10.1103/PhysRevD.55.6253 [arXiv:hep-ph/9606438 [hep-ph]].
- [212] P. Basler and M. Mühlleitner, Comput. Phys. Commun. **237** (2019), 62-85 doi:10.1016/j.cpc.2018.11.006 [arXiv:1803.02846 [hep-ph]].